

Versatile Experimental Kevlar Array Hydrophones: USRD Type H78

ALLAN C. TIMS
Transducer Branch

and

CRAIG K. BROWN
Electronics Branch

Underwater Sound Reference Detachment
P.O. Box 8337
Orlando, Florida 32856

PLEASE RETURN THIS COPY TO:

NAVAL RESEARCH LABORATORY
WASHINGTON, D.C. 20375
ATTN: CODE 2628

Because of our limited supply you are requested to return this copy as soon as it has served your purposes so that it may be made available to others for reference use. Your cooperation will be appreciated.

NDW-NRL-5070/2651 (Rev. 9-75)

April 5, 1979



NAVAL RESEARCH LABORATORY
Washington, D.C.

REPORT DOCUMENTATION PAGE		READ INSTRUCTIONS BEFORE COMPLETING FORM
1. REPORT NUMBER NRL Report 8288	2. GOVT ACCESSION NO.	3. RECIPIENT'S CATALOG NUMBER
4. TITLE (and Subtitle) VERSATILE EXPERIMENTAL KEVLAR ARRAY HYDROPHONES: USRD TYPE H78		5. TYPE OF REPORT & PERIOD COVERED Final report on this portion of the NRL Problem
		6. PERFORMING ORG. REPORT NUMBER
7. AUTHOR(s) Allan C. Tims and Craig K. Brown		8. CONTRACT OR GRANT NUMBER(s)
9. PERFORMING ORGANIZATION NAME AND ADDRESS Underwater Sound Reference Detachment Naval Research Laboratory P.O. Box 8337, Orlando, FL 32856		10. PROGRAM ELEMENT, PROJECT, TASK AREA & WORK UNIT NUMBERS NRL Problem S02-36
11. CONTROLLING OFFICE NAME AND ADDRESS Office of Naval Research Arlington, VA 22217		12. REPORT DATE April 5, 1979
		13. NUMBER OF PAGES 67
14. MONITORING AGENCY NAME & ADDRESS (if different from Controlling Office)		15. SECURITY CLASS. (of this report) UNCLASSIFIED
		15a. DECLASSIFICATION/DOWNGRADING SCHEDULE
16. DISTRIBUTION STATEMENT (of this Report) Approved for public release: distribution unlimited		
17. DISTRIBUTION STATEMENT (of the abstract entered in Block 20, if different from Report)		
18. SUPPLEMENTARY NOTES		
19. KEY WORDS (Continue on reverse side if necessary and identify by block number) Hydrophone design Ceramic materials Low-noise preamplifier Sonar equipment Transducer array Passive sonar High-pressure research		
20. ABSTRACT (Continue on reverse side if necessary and identify by block number) The development and design of prototype hydrophones for the Versatile Experimental Kevlar Array (VEKA), a distributed-sensor suspended cable system, and a 32-channel Ship-board Acoustic Receiving Amplifier (SARA) is presented. The approach was to design hydrophones which are specifically made an integral part of the free-flooded compliant cable during fabrication. The array design required the hydrophones to be mounted coaxially within the strength members of the cable and electrical conductors. The hydrophone is a high-sensitivity low-self-noise design. The design includes a custom-made hybrid microelectronic preamplifier		

DD FORM 1 JAN 73 1473

EDITION OF 1 NOV 65 IS OBSOLETE
S/N 0102-014-6601

i

SECURITY CLASSIFICATION OF THIS PAGE (When Data Entered)

20. Abstract (Continued)

mounted within the acoustic sensor element. The preamplifier uses a current-mode line driver to send the electrical signal up the VEKA cable to the SARA, where the signal is converted to a voltage and amplified prior to signal processing. Milestones of the hydrophone development were: design of a preamplifier system capable of driving 9200 m of cable in either a voltage or current mode (two-wire system); development and application of hybrid microelectronic circuits to noise-measuring hydrophones; and design of a unique remote switching circuit to provide calibration functions, hydrophone output signals, and hydrophone power on a two-wire system.

CONTENTS

INTRODUCTION	1
GUIDE SPECIFICATIONS FOR VEKA I HYDROPHONES	4
ACOUSTIC CONSIDERATIONS IN THE SENSOR	6
Sensor Material	6
Configuration	8
H78A HYDROPHONE DESIGN	9
Description of the Hydrophone	9
Sensor Theory	10
H78A CURRENT-MODE PREAMPLIFIER	11
PREAMPLIFIER OVERLOAD AND RECOVERY MEASUREMENTS	14
VEKA I-A CONE ADAPTERS	15
H78B EXPERIMENTAL HYDROPHONE	16
SHIPBOARD ACOUSTIC RECEIVER AMPLIFIER (SARA)	17
DEVELOPMENTAL ACOUSTIC MEASUREMENTS	23
H78A PREAMPLIFIER SELF-NOISE	28
DYNAMIC TEST OF PROTOTYPE CABLE AND PROTOTYPE HYDROPHONES	31
HIGH-STRESS EFFECTS ON RADIALY POLARIZED CAPPED CERAMIC CYLINDERS	35
CALIBRATION OF VEKA I-A HYDROPHONES	36
USRD TYPE H78D HYDROPHONE	39
Description	39
Cone Adapters	41

CONTENTS (Continued)

H78 VOLTAGE-MODE PREAMPLIFIER.....	42
CONCLUSION	43
ACKNOWLEDGMENTS.....	43
REFERENCES	43
APPENDIX A — Calculations of Sensitivity and Capacitance of Various Piezoelectric Sensors	45
APPENDIX B — H78A Reproducibility and Matching.....	48
APPENDIX C — H78B Current-Mode Preamplifier	50
APPENDIX D — Alternate Calibration Method	52
APPENDIX E — VEKA I-A Prototype Cable.....	57
APPENDIX F — Analysis of VEKA I-A Cable Failure	60

VERSATILE EXPERIMENTAL, KEVLAR ARRAY HYDROPHONES: USRD TYPE H78

INTRODUCTION

The Naval Ocean Research and Development Activity (NORDA) and the NRL Acoustics Division jointly tasked the NRL Underwater Sound Reference Detachment (USRD) to develop and construct prototype hydrophones and associated electronics for the Versatile Experimental Kevlar Array (VEKA I-A). The array program is a use of the cable technology provided by a program sponsored by the Naval Facilities Engineering Command during FY-1971 through FY-1975 [1]. A major objective of VEKA is to provide a wide-aperture distributed-sensor cable system with increased reliability, versatility, and performance using a free-flooded, lightweight, torque-free, compliant cable with hydrophones specifically designed for the cable environment when they are made an integral part of the cable during fabrication.

This report presents in detail the design considerations, tests, and evaluations conducted to provide a hydrophone design for VEKA I-A. Several milestones in the hydrophone development program are described in detail. Many of the developments were not used in the array hydrophones, even though they were deemed necessary at certain phases of the development program by the sponsors. They are reported here, however, because they constitute a significant part of the development effort and can have an impact on future hydrophone designs.

Milestones of the hydrophone development program were: design of a low-noise preamplifier system capable of driving 9200 m of cable in either a voltage or current mode (two-wire system), application of hybrid microelectronic circuits to low-noise hydrophones, design of a unique remote switching circuit to provide calibration functions for a two-wire preamplifier system, design of a unique calibration circuit which employs an optical isolator, and development of a low-cost expendable hydrophone for future VEKA considerations.

Figure 1 shows the array cable and sensors of the VEKA I-A in schematic form. Thirty-two USRD type H78A hydrophones spaced at 10-m intervals constitute the main acoustic array. Three engineering sensor stations (one at the top of the array, one at the center, and one at the bottom) provide pressure and temperature monitoring. The station housings were designed by USRD, and the pressure transducers and thermistors were provided by NORDA. At the lower end of the array are six experimental hydrophones for evaluation for future arrays. Some of the experimental hydrophones were designed by USRD and are described in subsequent sections of this report. All of the hydrophones and the engineering stations are mounted coaxially within the Kevlar main-array cable, with each being enclosed by a smooth bulge in the polyester overbraid. Figures 2 and 3 show the array deployed in vertical and horizontal configurations respectively. The Kevlar main-array cable and umbilical were designed, developed, and provided by NORDA and contractors [2].

Manuscript submitted November 8, 1978.

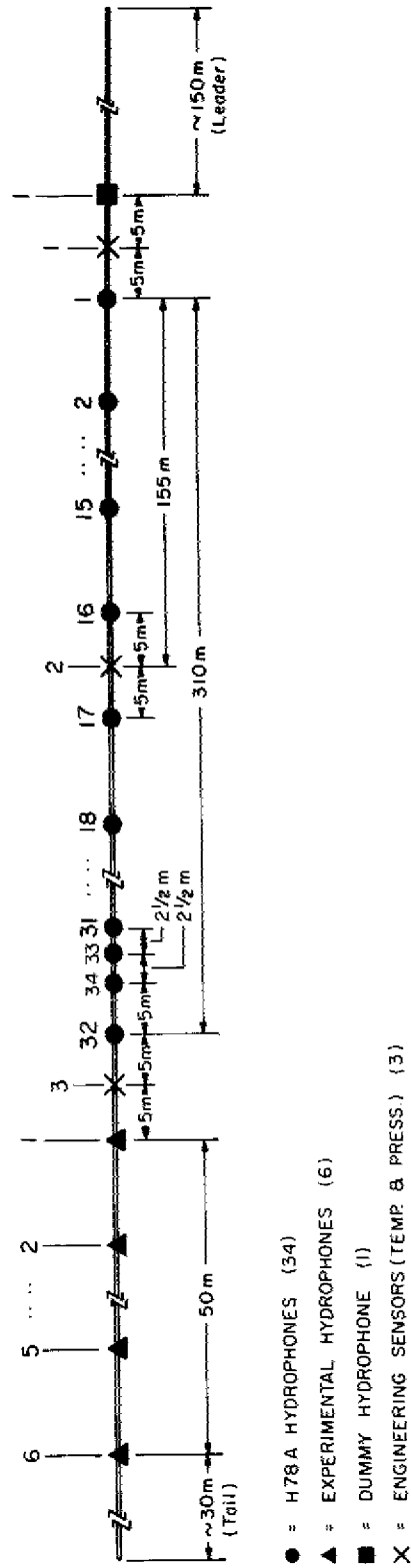


Fig. 1 -- Schematic diagram of the VEKA I-A

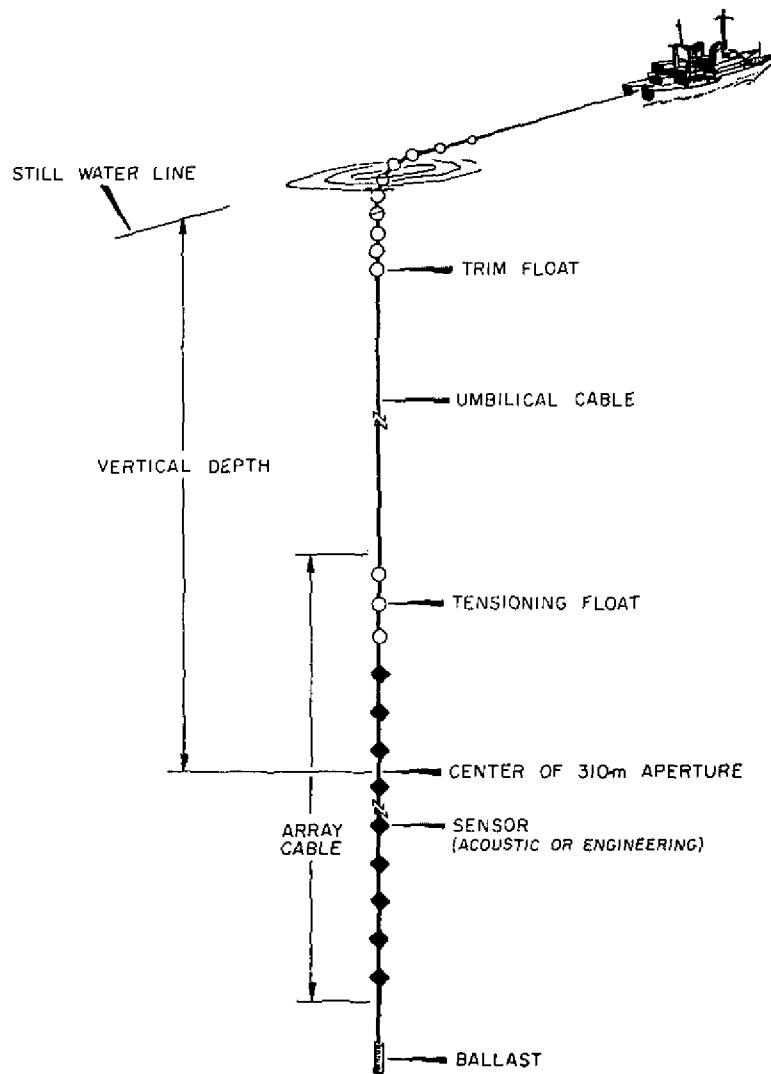


Fig. 2 — Vertical configuration of the array

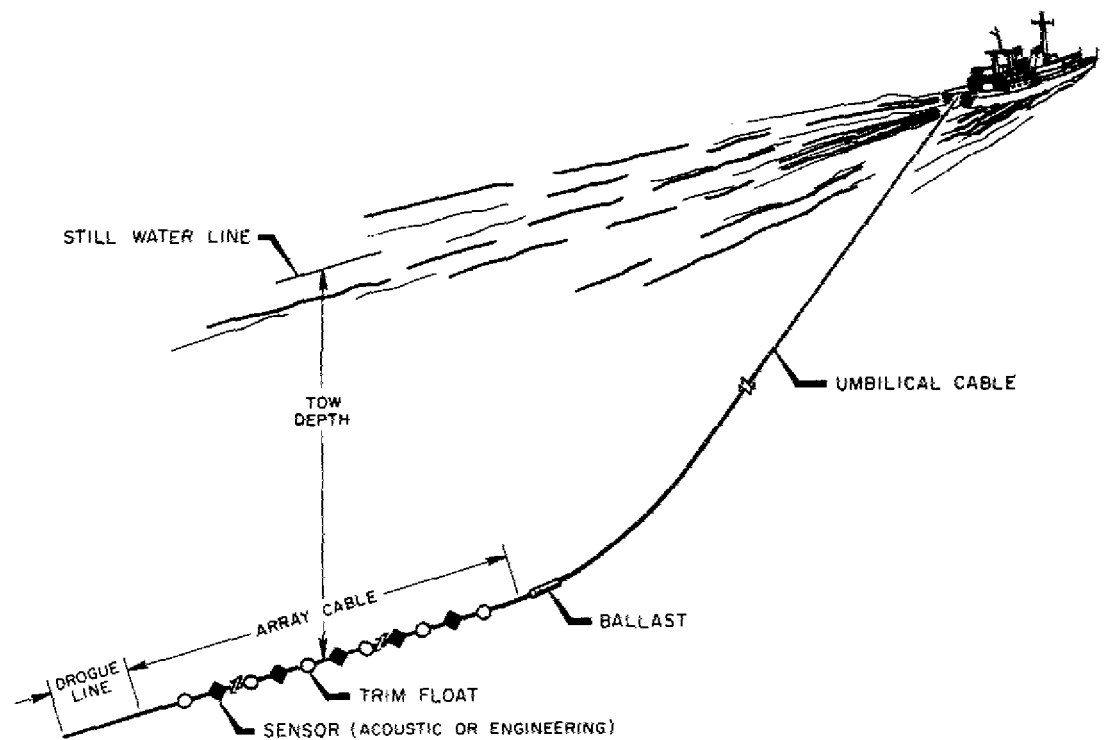


Fig. 3 — Horizontal configuration of the array

GUIDE SPECIFICATIONS FOR VEKA I HYDROPHONES

Guide specifications provided by the program sponsors were as follows. The environmental requirements were:

Pressure capability: 0 to 68.9 MPa,

Temperature range: - 4 to +40°C.

The acoustical-electrical requirements were:

Sensitivity: -186 dB re 1 V/ μ Pa open-circuit crystal sensitivity or better,

Frequency response: 0.5 dB from 2 Hz to 2 kHz or higher,

Directivity: omnidirectional within 0.5 dB over the frequency range,

Acceleration response: canceling along the vertical axis,

Preamplifier: may have unity gain or greater, and the output must be able to drive 9200 m of No. 24 AWG wire,

Equivalent noise pressure: 10 dB less than Knudson's sea-state-zero over the frequency range, with the low-frequency range as good as or better than the plot shown in Fig. 4,

Dynamic range: 60 dB or greater,

Calibration circuit: calibration capability must exist by injecting a signal into the input of the preamplifier on a separate calibration line, by sending the signal on the power line, or by an internally generated signal.

The mechanical requirements were:

Mass: 0.45 kg or less in water,

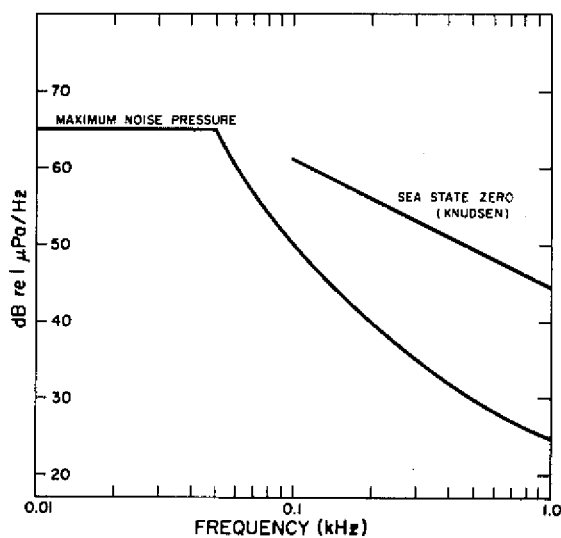
Maximum length: 10 cm,

Maximum diameter: 3.8 cm,

Preamplifier location: accessible for modifications as necessary,

Cables and connectors: 15 to 20 cm long with single-pin male Mecca-type connectors.

Fig. 4 — Guide specification for equivalent noise pressure



The array design required the hydrophones to be mounted coaxially within the cable without damaging the strength members of the cable or the electrical conductors. The design also required that the hydrophones not be subjected to compressive forces as a result of tension or bending in the cable. During deployment of the array the hydrophone must be able to pass over a 1.2-m-diam sheave with a tension as high as 4450 N in the cable without damage to the hydrophone or the cable.

The order in which the items appear in this specification is not an indication of their relative importance. Other requirements that are not explicitly stated are important, such as long operational lifetime and sufficient ruggedness to withstand field use under adverse circumstances. Low cost was also considered a requisite, because many hydrophones are needed for the array and for possible future VEKA arrays.

ACOUSTIC CONSIDERATIONS IN THE SENSOR DESIGN

In the design of a small deep-submergence noise-measuring hydrophone for the infrasonic and low-audio frequency range, three hydrophone characteristics, sensitivity, depth capability, and self-noise, are usually the key parameters. The exact natures of these parameters are determined by the material selected for the sensor and its configuration. It is generally understood in the art that the sensitivity and depth capabilities are determined by the sensor material and its configuration. Not so well understood is that the self-noise of a hydrophone is also largely determined by the sensor, particularly so when a modern low-noise JFET is used for the input stage of the preamplifier. The sensor contributes to the noise of the system by the amount of impedance loading on the first stage of the preamplifier. Ideally the sensor material and its configuration must have characteristics that give good sensitivity, must be able to withstand high hydrostatic stress without significant change in sensitivity, and must have sufficient capacitance to impedance-load the preamplifier input stage to reduce the self-noise to a minimum.

Sensor Material

Lithium Sulfate

Lithium sulfate would usually be an excellent choice for use as the sensor material in this application because of its good sensitivity as a volume expander, its stability with time, its outstanding depth capability, and its predictable characteristics [3,4]. But the volume of material required to provide adequate capacitance and the cost of the material itself prohibit its use in this design. Appendix A contains calculations of the sensitivity and capacitance of lithium sulfate.

Lead Metaniobate

Following lithium sulfate the next best sensor material with stable characteristics in high-pressure applications is lead metaniobate. Measurements made at USRD indicate that lead metaniobate will decrease in sensitivity about 1.5 dB at pressures to 68.9 MPa [5].

The only practical configuration for a lead-metaniobate sensor is a disk, a rectangular plate, or a length-polarized cylinder because of its low g_{31} piezoelectric constant. Radially polarized cylinders and spheres are g_{31} -dependent configurations and thus are impractical configurations for the material.

A disk 1.85 cm thick operating in a hydrostatic mode would have the required minimum sensitivity given in the guide specifications; however, it would be too thick and probably could not be adequately polarized. Two disks 0.93 cm thick would have to be bonded together in series for the required thickness. Eight crystals bonded together in a series-parallel combination would have a sensitivity of -186 dB re 1 V/ μ Pa, and if they were 2.5 to 3 cm in diameter, the capacitance would range from 240 to 340 pF, depending on the exact diameter. A capacitance of 500 to 600 pF would be more desirable for this application and would lower the noise floor about 6 dB [6] below the noise of a 240-to-340-pF sensor. The total length of the assembled stack would be 7.4 cm, which takes up 74% of the allowable length for the hydrophone and leaves only 2.6 cm for the preamplifier and cable connections. Lastly, the cost of the lead metaniobate material would be about 3 times or more that of lead zirconate titanate crystal. Thus, because of low capacitance, marginal sensitivity, space limitations, and cost, it was decided that lead metaniobate was not practical for this design. Appendix A gives an example of sensitivity and capacitance calculations.

Lead Zirconate Titanate

Good sensitivity, low cost, and high dielectric constant are the general characteristics of a family of piezoelectric materials of lead zirconate titanate composition. Some of these materials are defined by MIL STD 1376 (SHIPS) [7] as Navy type I, II, and III compositions. There is little difference in the piezoelectric constants of these materials; therefore the sensitivity for a given configuration will be about the same. The primary considerations in their use are pressure stability and dielectric constants. The type II material has the highest dielectric constant but is not suitable for high-pressure applications. The type I material has a moderately high dielectric constant and has been used with good results in a spherical configuration at hydrostatic pressures to 68.9 MPa [5,8]. Transducer and hydrophone designs tend to favor the type I material at hydrostatic pressures greater than 5 or 6 MPa. The type III material is a high-drive, high-stress ceramic and has the lowest dielectric constant of the three. But its dielectric constant, even though low compared to those of the type I and II materials, is 4 times greater than that of lead metaniobate and 100 times greater than that of lithium sulfate.

Configuration

To use the characteristics of these materials to their fullest potential, a hollow sphere or cylinder that is radially polarized is required for the sensor. A sphere with a diameter-to-wall-thickness ratio of 8 using the type-I material would experience a reduction in sensitivity of about 1.5 dB at pressures to 68.9 MPa [5]. Appendix A gives an example of sensitivity and capacitance calculations. A sphere 3.5 cm in diameter with a 4.4-mm wall has a theoretical sensitivity of -196.2 dB re $1 \text{ V}/\mu\text{Pa}$ and a capacitance of 7530 pF. If the sphere were quartered and the segments wired in series, the theoretical sensitivity would be -184.2 dB with a capacitance of 1883 pF. This would be a good sensor adequately meeting the guide specifications in most areas except low cost. The cost of a sphere, actually hemispheres bonded together, and the subsequent sectioning and reassembly would make the cost of the sensor prohibitive. Recent purchases of radially polarized cylinders 3 cm in diameter with a 4.8-mm wall thickness and 1.27 cm long cost \$6.00 each. In contrast, hemispheres 2.54 cm in diameter with a 3.1-mm wall thickness cost \$96.00 a pair.

A radially polarized capped cylinder has adequate sensitivity to meet or exceed the guide specifications and is low in cost. However, its sensitivity is a function of depth. Capped cylinders experience essentially two-dimensional stresses which can be far greater than the hydrostatic pressure. The same mechanical transformation that yields the increased sensitivity to sound also multiplies the hydrostatic pressure. These two-dimensional stresses affect the piezoelectric and dielectric constants of the ceramic and can result in complete depolarization of the material. Work has been done to determine the compressive stress limits (one-dimensional) for the type I, II, and III materials [9]. Unfortunately data on the effects of stress on the ceramic cylinders are completely inadequate. Also it is not well understood how the individual components of stress combine to represent the resulting stress which leads to changes in sensitivity, dielectric constant, and/or depolarization. But empirical data strongly suggest that ceramics resist changes from a two-dimensional stress more than from a one-dimensional stress.

When a cylindrical sensor is used with the dimensional constraints and limitations imposed by the guide specifications, sensitivity stability at great depth is sacrificed to increase the overall sensitivity and to provide sufficient capacitance to insure a low self-noise. In most instances the VEKA array would be used at depths less than 5 to 6 km. Thus, in the VEKA design, increased sensitivity and a lower noise floor are more important than stability at great depths. Another advantage of the cylindrical design is that the preamplifier can be placed inside the sensor element, with the end caps forming a pressure housing for the electronics. With this advantage the allowable external dimensions of the hydrophone can be virtually filled with sensing material and still retain adequate space for the electronics. Obviously, when this design is used, the preamplifier does not need pressure-hardened components.

H78A HYDROPHONE DESIGN

Description of the Hydrophone

The H78A hydrophone is shown in a sectional view in Fig. 5. The sensitive elements are of type I material, have a 3.0-cm o.d., 2.05-cm i.d., and 1.27-cm length, and are bonded together with Epon VI industrial epoxy and electrically wired in series. Adjacent crystals are polarized in opposite directions, which simplifies the wiring of the element. Figure 6 is a view of the crystal assembly showing the electrode connections. Bonded to one end of the crystal assembly is an end cap of 98%-pure aluminum oxide. Bonded to the other end of the crystal assembly is an end ring which receives a cable-gland assembly and thus forms the other end cap.

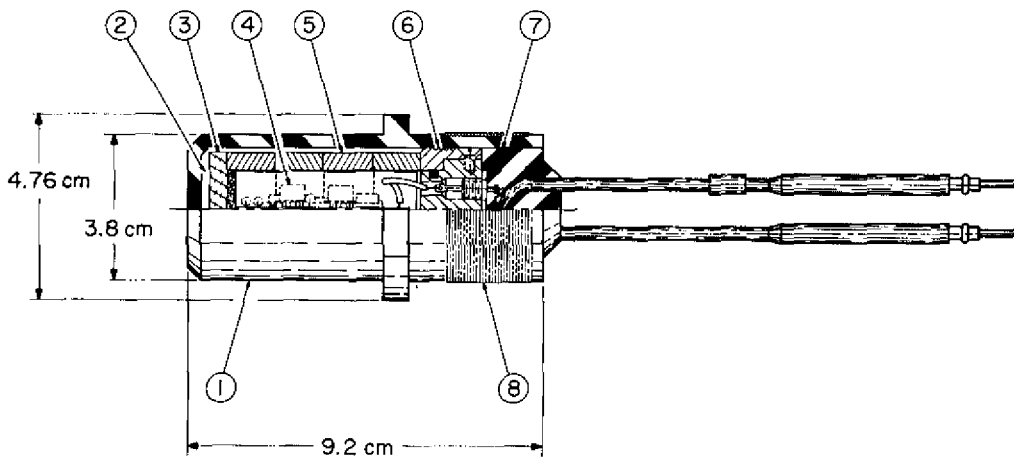


Fig. 5 — USRD type H78A hydrophone: (1) butyl rubber boot with integral mount ring, (2) coupling fluid, (3) aluminum oxide end cap, (4) preamplifier, (5) ceramic sensor, (6) end ring, (7) cable assembly, and (8) banding

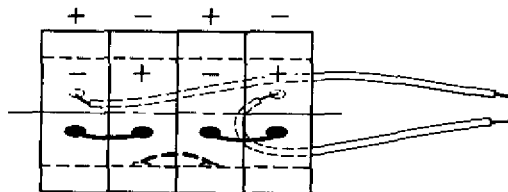


Fig. 6 — Crystal assembly and electrode connections

The cable-gland assembly receives the single-conductor cables with Mecca-type single-pin connectors. The cables are soldered to two high-pressure hermetic seals. The seals are enclosed in neoprene rubber, which is vulcanized and bonded to the cables and the cable gland. The cable assembly is sealed in the end ring by an O-ring and secured with flathead screws. The end ring and cable gland are made of type 316 stainless steel.

Inside the sensor assembly is the preamplifier, which operates in a current mode. The preamplifier is constructed on a 1.6-mm (1/16-in.) fiberglass circuit board using a custom-designed hybrid microelectronic circuit and other discrete components.

A sulfur-free electrical-grade butyl-rubber boot with an integral mount ring encloses the sensor-and-cable-gland assembly. Butyl rubber is used for the boot to ensure stable performance characteristics during prolonged continuous submergence. The mount ring is at the longitudinal center of mass to minimize the acceleration response in the vertical plane. Castor oil, thoroughly dried and degassed, serves as the coupling medium between the sensitive elements and the boot. Nylon banding seals the assembly in the boot, which constitutes a double watertight seal between the water and the preamplifier. All metal parts are isolated from the water, which prevents electrical ground loops and deterioration in saltwater.

Sensor Theory

The sensitive element chosen for the H78A hydrophone is a radially polarized piezoelectric cylinder of type I material. Four cylinders are bonded together and electrically wired in series to provide the desired sensitivity. The sensor configuration operates in an ends-capped mode. The expression for the sensitivity in terms of the ratio of voltage e to pressure p has been derived by Langevin [10] and is

$$\frac{e}{p} = b \left[g_{33} \frac{(1-\rho)}{(1+\rho)} + g_{31} \frac{(2+\rho)}{(1+\rho)} \right], \quad (1)$$

where g_{33} and g_{31} are the piezoelectric constants of the ceramic material, b is the outer radius of the cylinder, and ρ is the ratio a/b , where a is the inner radius of the cylinder.

The capacitance is [10]

$$C = \frac{2\pi K_{33}^T \epsilon_0 \ell}{\ln(b/a)}, \quad (2)$$

where b and a are as defined above, ℓ is the length of the cylinder, K_{33}^T is the relative dielectric constant, and ϵ_0 is the permittivity of free space.

The dimensions of the ceramic element are inner radius $a = 1.03$ cm, outer radius $b = 1.508$ cm, and length $\ell = 1.27$ cm. Nominal values for the electromechanical voltage constants are $g_{33} = 24.5 \times 10^{-3}$ V·m/N and $g_{31} = -10.7 \times 10^{-3}$ V·m/N and the value of the relative dielectric constant K_{33}^T is 1300.

Substituting in equation 1 the appropriate values for the ceramic material and $p = 1 \mu\text{N}/\text{m}^2 = 1 \mu\text{Pa}$ gives $e/p = 1.876 \times 10^{-10} \text{ V}/\mu\text{Pa}$. Expressed in dB, $M = -194.5 \text{ dB re } 1 \text{ V}/\mu\text{Pa}$, where M is the free-field voltage sensitivity of a single capped element when its dimensions are small in comparison with the wavelength.

For four crystals electrically wired in series the increase in sensitivity is $20 \log 4$ or 12 dB, which gives $-182.5 \text{ dB re } 1 \text{ V}/\mu\text{Pa}$ as the theoretical free-field voltage sensitivity for the H78A sensor. Some reduction in sensitivity can be expected due to fringe capacitance between the element electrodes: about 0.5 dB. Some loss may also result from the clamping effect of the end caps, because they are bonded to the elements by a rigid epoxy [11]. Expected losses should not exceed 1 dB.

Substituting the appropriate values in equation 2 gives a theoretical capacitance of 2408 pF. For the four elements in series the theoretical capacitance is $C = 602 \text{ pF}$. (Variations in the actual values were balanced off in selecting elements for each series, so that the various series would have little variation between them, as described in Appendix B.)

H78A CURRENT-MODE PREAMPLIFIER

The preamplifier used in the H78A hydrophone is shown schematically in Fig. 7. This design can drive a No. 24 AWG twisted-pair cable up to 9200 m long over a frequency range of 10 Hz to 10 kHz. The lower cutoff frequency is determined by the capacitance of Y1 (nominally 635 pF) and the input impedance of A1 (25 M Ω). The high-frequency limit is determined by the capacitance between cable conductors.

The preamplifier input comes directly from the hydrophone crystal Y1. Diodes CR3 and CR4 protect the preamplifier from input transients and prevent a buildup of dc charge on the crystal.

Hybrid circuit A1 is a low-noise preamplifier specifically designed during the hydrophone development program for VEKA application. It has a voltage gain of 20 dB and operates from +12 V dc established by zener diode CR2. Figure 8 is a schematic diagram of A1. NRL report 8218 [12] presents both a dc and low-frequency ac analysis of this type of amplifier configuration, so this will not be repeated here.

The preamplifier output uses a twisted pair of No. 24 AWG wires in the VEKA cable. It terminates at the SARA receiver (described in a later section of this report) where point A (Fig. 7) is connected to +36 V dc and point B is connected to a 40.2- Ω load resistor. Both the dc supply current to the preamplifier and the ac signal current from it share the single wire pair. Current flows into the preamplifier at point A and out at point B.

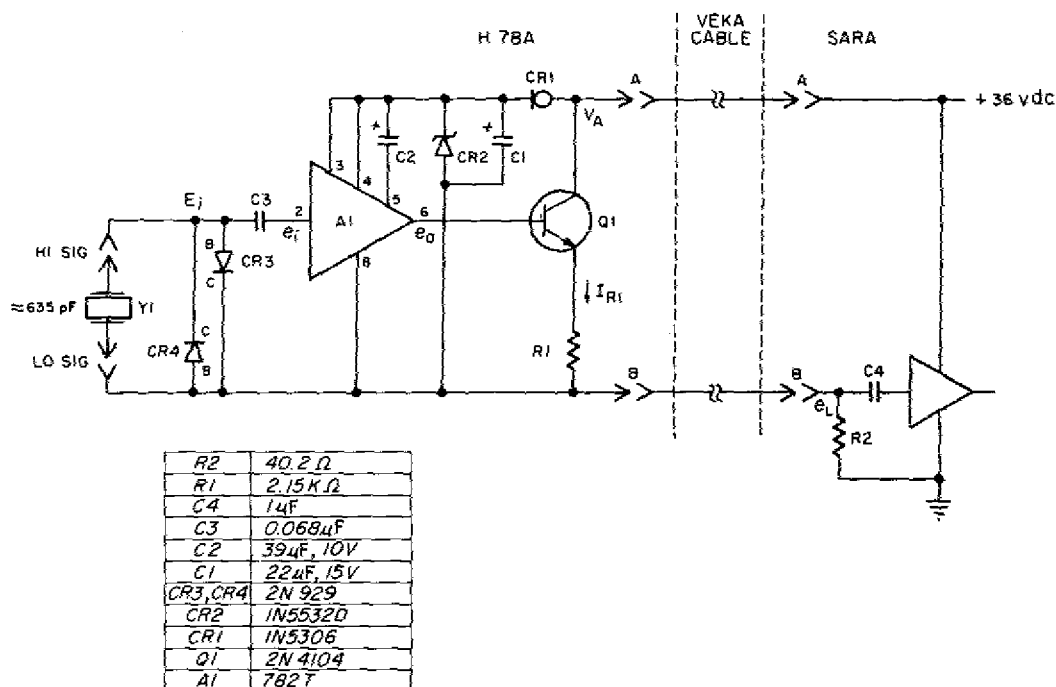


Fig. 7 — Schematic of the H78A preamplifier showing the interface to SARA (one channel)

Current-regulator diode CR1 supplies a constant 2.2 mA to CR2 and A1. A second current regulator, made up of Q1 and R1, converts A1's output voltage into output current I_{R1} . This current has a 1.8-mA dc component and an ac component equal to $e_o/R1$, where e_o is the audio output voltage of A1. The ac voltage developed across the 40.2-Ω load resistor R2 is therefore

$$e_L = e_o \left(\frac{R2}{R1} \right). \quad (3)$$

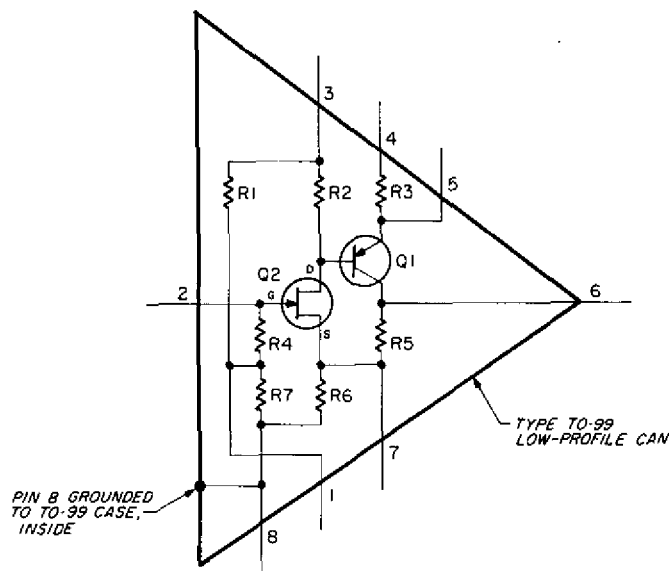
If e_i is the input voltage at pin 2 of A1 and G is the voltage gain of A1, then

$$e_L = G e_i \frac{R2}{R1}. \quad (4)$$

Hence the overall gain of the preamplifier is

$$\frac{e_L}{e_i} = \frac{R2}{R1} G. \quad (5)$$

The dc-current values just mentioned are nominal, and they develop a dc voltage across the 40.2-Ω load. This dc component is blocked by coupling capacitor C4 at the input of the SARA receiver.



$R1 = 510K\Omega$
 $R2 = 13K\Omega$
 $R3 = R7 = 9.1K\Omega$
 $R4 = 25 \times 10^6\Omega$
 $R5 = 15K\Omega$
 $R6 = 1.5K\Omega$
 $Q1 = 2N3251A \text{ CHIP}$
 $Q2 = 2N4867A \text{ CHIP}$

Fig. 8 — Integrated circuit A1 used in the H78A hydrophone preamplifier

Noise tests and transient response characteristics of this circuit are given in a later section of this report. Other typical performance is given in Table 1.

Table 1 — Typical Performance of the H78A Preamplifier

Input impedance	$25 M\Omega \pm 5\%$
Input voltage (for linear operation)	0.2 V rms max
Bandwidth (for zero cable length)	100 kHz
Lower cutoff frequency (-3 dB)	10 Hz
Gain (for a load of 40.2Ω)	-14.5 dB
Dynamic range	100 dB
Supply voltage	+20 to +38 V dc
Supply current	2.9 to 5.7 mA dc

PREAMPLIFIER OVERLOAD AND RECOVERY MEASUREMENTS

In the design of the H78 preamplifier, CR3 and CR4 were added to protect the preamplifier from input transients or overloads that could damage the input FET. With the preamplifier as shown in Fig. 7 and a 635-pF capacitor substituted for the sensor element, the following overload test was conducted.

Through a gating system a 12-V dc overload pulse coincident with a 100-mV sine wave was applied to the input of the preamplifier. This scenario corresponds to a pulse SPL (sound pressure level) of about 205 dB re 1 μ Pa followed by a steady-state signal of 164 dB. Under this condition the preamplifier was overloaded more than 46,000 times over a 5-hour interval to establish long-term reliability.

The preamplifier output and recovery time is shown in Fig. 9; a Biomation model 610 transient recorder was used to capture and record the preamplifier output. The recovery time measured is nominally 60 μ s.

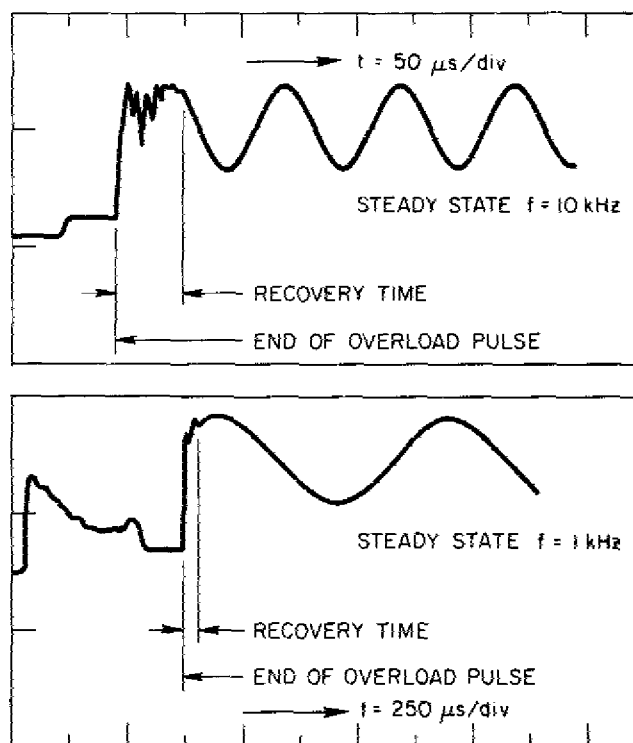


Fig. 9 — Preamplifier recovery time

The 2N929 pn junctions used for CR3 and CR4 start to conduct at about 425 mV; two will provide adequate preamplifier protection for SPLs up to 218 dB (50 V). If higher levels are expected, junctions can be added in series.

VEKA I-A CONE ADAPTERS

The H78A, H78C, and H78E hydrophones require an adapter to fair the hydrophones into the VEKA cable. The purpose of the adapter is to provide a smooth low-profile bulge in the cable that secures and protects the hydrophones, allowing reasonable flexibility and bending of the cable without damaging the cable strength members. The cone adapters are similar to those used for the ITC model 8021 hydrophones in the Moored Acoustic Buoy System (MABS) [1]. However, the VEKA adapters are noticeably smaller (60% by volume), and a sensor cage is not required for the hydrophones. Figure 10 shows the MABS-type cone adapter and the new VEKA cone adapter. The MABS cone has a nominal mass of 1.86 kg, and the VEKA adapter has a nominal mass of about 0.76 kg.

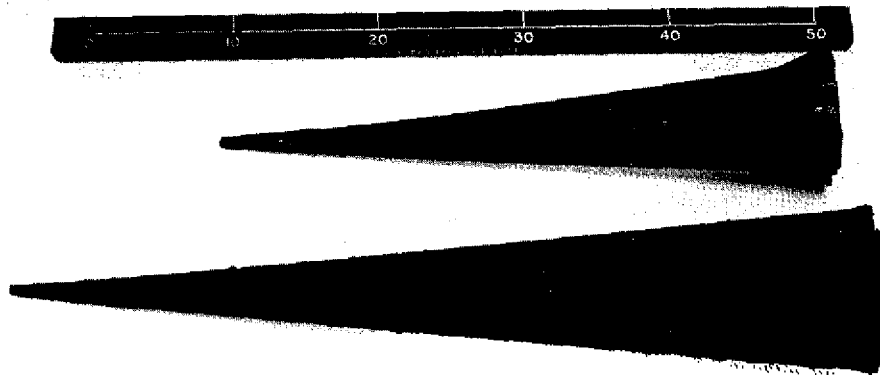


Fig. 10 — MABS cone adapter (bottom) and a VEKA I-A cone adapter (next to the centimeter scale)

Figure 11 is a drawing showing an H78A hydrophone within a set of cone adapters. Each cone has a type 316 stainless-steel ring with a periphery that accepts the mount ring on the boot of the hydrophone. A butyl rubber (USRD compound 70821) vulcanized and bonded to the rings forms a fairing for the hydrophone. Four stainless-steel 1/4-20 cap screws, two in each cone 180° apart, hold the assembly together.

Figure 12 shows a cone adapter and hydrophone installed in a section of VEKA prototype cable. In fabrication of the array cable the adapters were installed in the cable, wired, and then overbraided with a polyester braid.

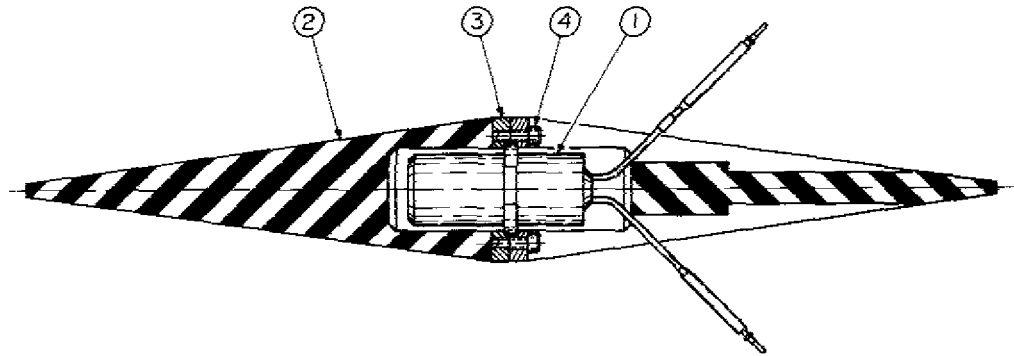


Fig. 11 — H78A hydrophone in a cone adapter set: (1) H78A hydrophone, (2) butyl rubber cone, (3) stainless-steel rings, and (4) cap screw.



Fig. 12 — Hydrophone and cone assembly installed in the VEKA I-A prototype cable

H78B EXPERIMENTAL HYDROPHONE

From the standpoint of the sensor element and receiving sensitivity, the H78B is the same as the H78A. A sectional view of the B model is shown in Fig. 13. The overall design follows the concept of an integrated cone-adapter-and-sensor assembly. The capped-cylinder sensor is enclosed in an expanded metal frame that is acoustically transparent and imparts exceptional ruggedness to the hydrophone. The sensor element is positioned within the frame at its longitudinal center of mass in an elastomer mount ring. The preamplifier is enclosed in an accessible pressure housing. A major difference with the B model is the calibration circuit. A calibration capability by injecting a signal into the input of the preamplifier on a separate calibration line or by an internally generated signal was in the original guide specifications. This hydrophone has the calibration capability in a unique circuit, which is described in Appendix C. (An alternate calibration circuit is described in Appendix D.) The calibration-circuit provision was eventually dropped by the program sponsors in lieu of a simplified hydrophone.

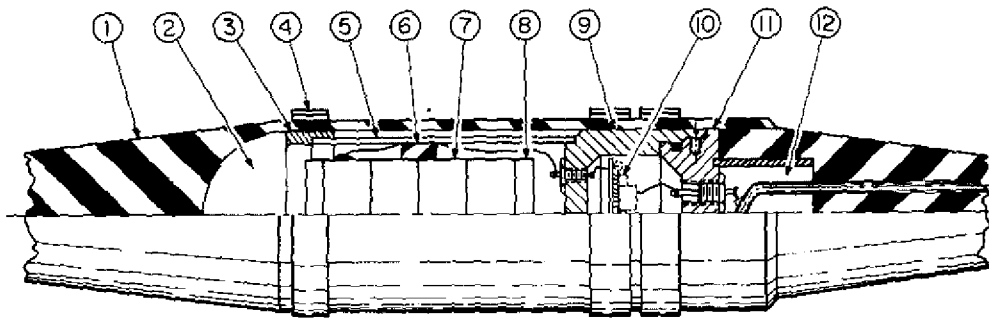


Fig. 13 — Sectional view of USRD type H78B hydrophone: (1) integral butyl boot and cone adapter, (2) castor-oil coupling fluid, (3) frame end ring, (4) banding, (5) expanded metal frame, (6) elastomer sensor mount, (7) ceramic sensor, (8) aluminum oxide end cap, (9) preamplifier housing, (10) preamplifier, (11) cable gland with butyl cone, and (12) potting compound

SHIPBOARD ACOUSTIC RECEIVER AMPLIFIER (SARA)

The SARA electronics consist of

- 32 receiver amplifiers for the 32 hydrophones of the VEKA I array,
- four receiver amplifiers for experimental hydrophones, and
- a calibration signal generator.

Figure 14 shows the front panel of the SARA unit, Fig. 15 shows the back panel, and Fig. 16 shows the unit with the top cover removed. All of the 36 receiver amplifiers are identical. *There are four amplifiers per printed-circuit (pc) card in the chassis.*

Inputs to the 32 channels of VEKA I are made through the VEKA-I input connector on the front panel (lower right in Fig. 14). These inputs normally come from the array but may come from a test oscillator. A special SARA calibration cable has been provided for this purpose. The 32 receiver outputs are terminated at the OUTPUT TO APS front-panel connector (lower left in Fig. 14) and two PARALLEL OUTPUT connectors on the back panel (lower left in Fig. 15).

The four channels for experimental hydrophones are on a single card and are labeled A through D. Inputs to these four channels are made *either* through the AUX front-panel connector (lower right center in Fig. 14) *or* through the four BNC connectors in the column at the upper right center on the front panel. (The inner pin of each BNC connector goes to a 40.2- Ω input resistor, and the outer shell of the connector is grounded.) The outputs of these four channels are terminated in the BNC connectors in the column at the far right on the front panel.

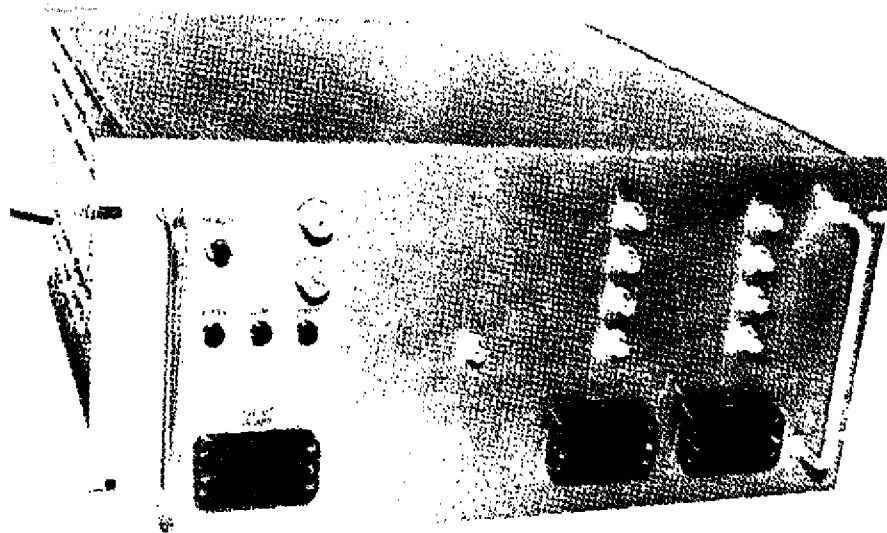


Fig. 14 -- Front panel of SARA



Fig. 15 -- Back panel of SARA

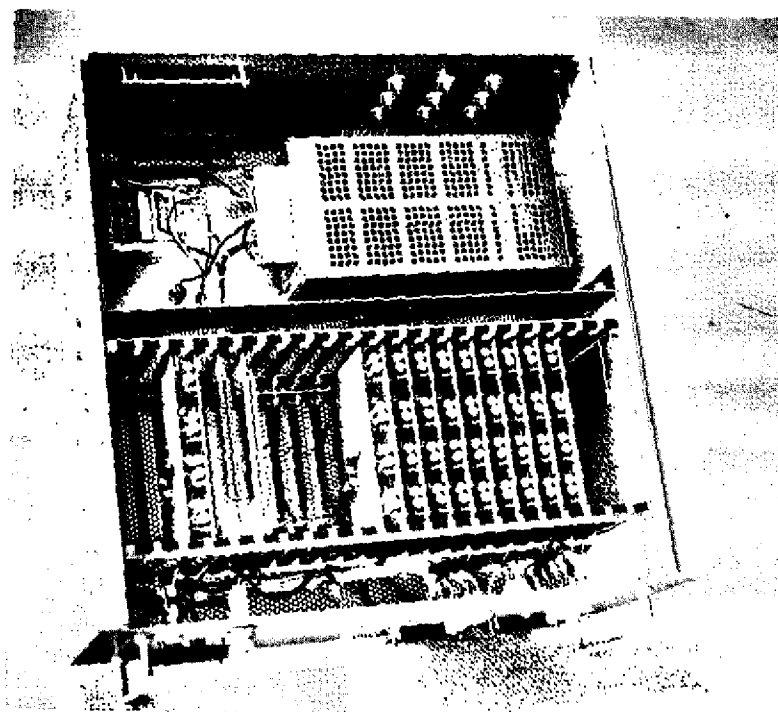


Fig. 16 — Top view of the SARA chassis

Because each SARA receiver card contains four independent and identical audio amplifiers, only one channel will be described here. A schematic diagram of one receiver channel is shown in Fig. 17. Input terminals A and B connect to points A and B respectively on the hydrophone preamplifier (Fig. 7) via a No. 24 AWG shielded twisted-pair cable. The cable shield is connected to power-supply ground at terminal S.

Terminal A furnishes current to the hydrophone preamplifier from the +36-V dc supply. The current is returned through terminal B to load resistor R2. The voltage drop across R2 has a dc bias plus an ac signal component. Capacitor C4 blocks the dc and couples the audio signal into hybrid amplifier circuit A1. Amplifier A1 has an input impedance of about 1 M Ω and a voltage gain of approximately 34 dB. Its output is available at test point TP1.

The output of A1 is further amplified by operational amplifier A2. This stage has unity dc gain and about 33 dB of ac gain. Provision is made on the card for optional line driver A3. This unity-gain buffer is presently omitted and replaced by a jumper. The output of A2 (or A3) is coupled by C7 to the card output test point TP2. The frequency response of the entire circuit is essentially flat from 10 Hz to 10 kHz.

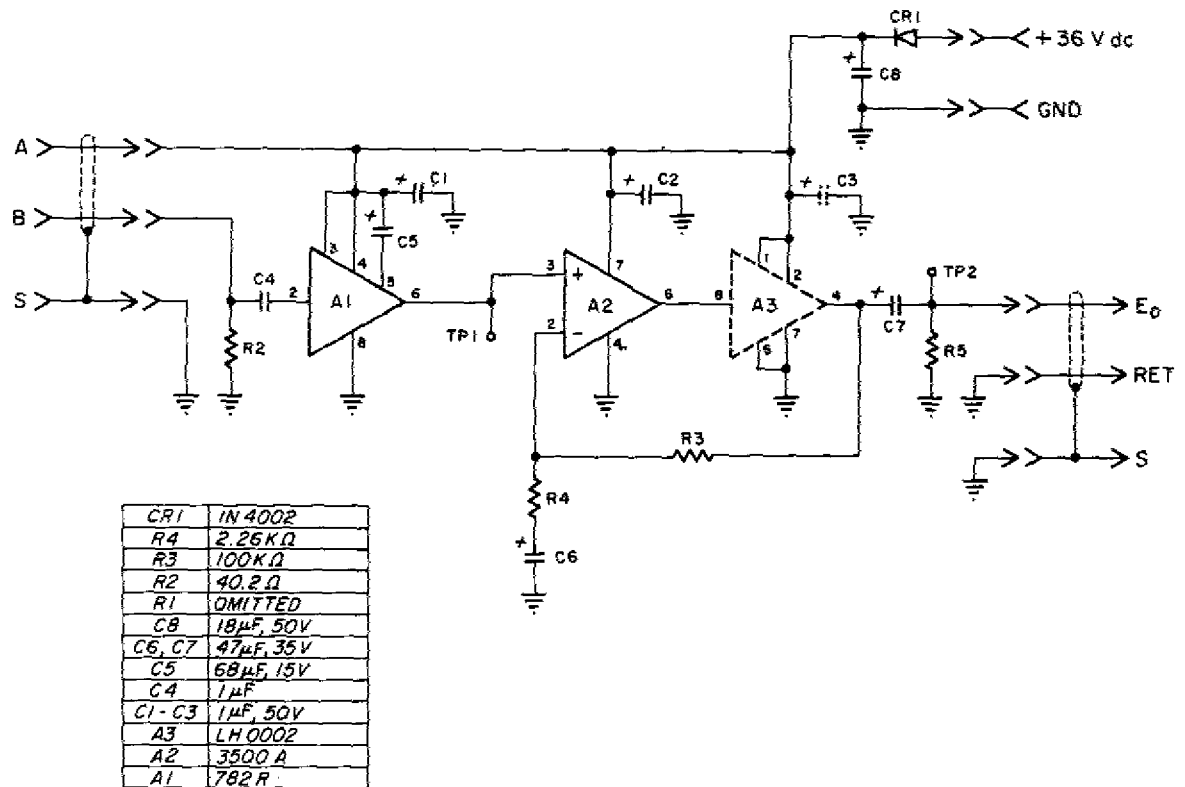


Fig. 17 — One channel of SARA

Hybrid circuit A1 (Fig. 18) is a low-noise amplifier specifically designed during the development program for VEKA application. The configuration of this device is the same as the hybrid circuit used in the H78A hydrophone preamplifier (Fig. 8), although the component values are different. Again, reference 12 provides complete design criteria for the circuit.

Table 2 gives the performance of a SARA receiver amplifier.

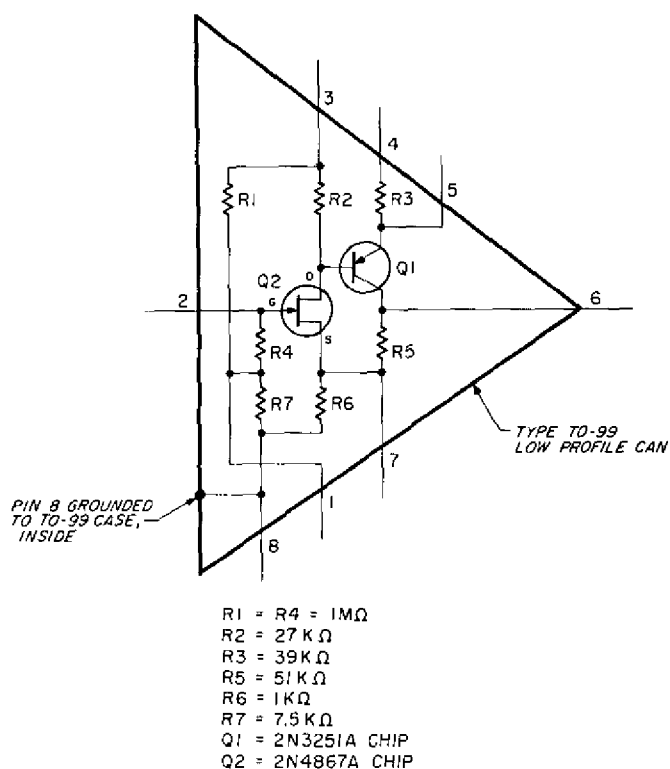


Fig. 18 — Integrated circuit A1 for SARA

Table 2 — Typical Performance of a SARA Receiver Amplifier

Supply current (per channel)	
Without line driver:	4.3 mA dc
With line driver:	10.3 mA dc
Input impedance	40.2 Ω
Input voltage (for linear operation)	2 mV rms max (-54 dBV)
Bandwidth (flat)	10 Hz to 10 kHz
Gain	67.2 \pm 0.5 dB
Output impedance	
Without line driver:	150 Ω in series with 47 μ F
With line driver:	6 Ω in series with 47 μ F
Dynamic Range (with H78A hydrophone preamplifier)	84 dB
Dc supply voltage	+36 \pm 5% V dc

The calibration signal generator is on a single card. Its input comes from an external test oscillator and is made at the CAL INPUT BNC connector at the center on the front panel. Its output is brought to the AUX front-panel connector at the lower right center and is enabled by turning on the CAL ON toggle switch at the lower right on the front-panel. A schematic diagram of the calibration signal generator is shown in Fig. 19. This circuit provides a controlled calibration current I_0 to the experimental H78B hydrophone preamplifier. It was originally intended to drive 32 such units in series, as indicated in Fig. 19.

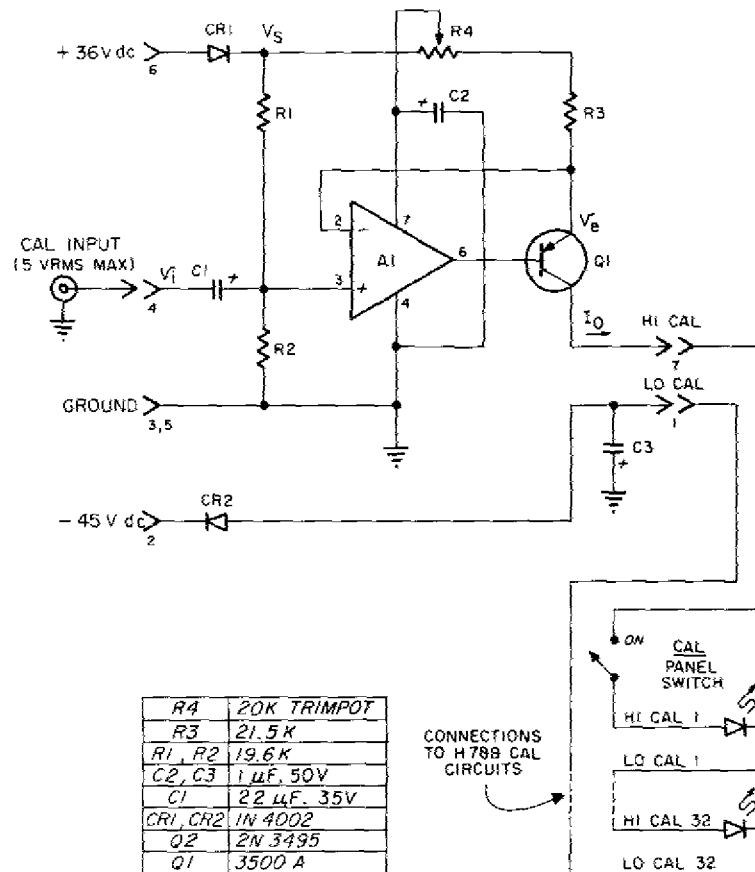


Fig. 19 — Calibration signal generator for SARA

Components Q1, R3, and R4 make up a current regulator. The collector current of Q1 is the calibration current I_0 delivered to the preamplifier. Operational amplifier A1 controls Q1's emitter voltage V_E .

As indicated by Fig. 19,

$$v_e = v_i + \frac{V_s R_2}{R_1 + R_2} = v_i + \frac{V_s}{2}$$

and

$$I_0 \approx \frac{V_s - v_e}{R_3 + R_4} = \frac{0.5V_s - v_i}{R_3 + R_4}.$$

It is seen from the preceding equation that I_0 has both an ac and a dc component. Resistor R_4 is variable, allowing I_0 to be trimmed. Appendix C of this report explains the circuitry which uses current I_0 .

Table 3 gives some typical performance parameters for the calibration signal generator.

Table 3 — Typical Performance of the
SARA Calibration Signal Generator

Input impedance	9.8 k Ω
Input voltage	5 V rms max
Bandwidth (flat)	10 Hz to 10 kHz
Gain (ac)	36 μ A/V
Supply voltage	36 \pm 5% V dc
Supply current	5.1 mA dc

DEVELOPMENTAL ACOUSTIC MEASUREMENTS

During the development of the H78 hydrophones several calibration measurements were made on experimental prototypes to determine the effect of the cone adapters and the VEKA-I cable on the acoustic response. Measurements were also made to assure the effective frequency range and directivity of the design. The measurements presented were made in the USRD Lake Facility.

Figure 20 shows the typical free-field voltage sensitivity (FFVS) of an H78A. This curve is for the hydrophone (no cone adapters) with a 12-m two-conductor shielded test cable. The upper limit of the usable frequency range for the hydrophone is about 12 kHz.

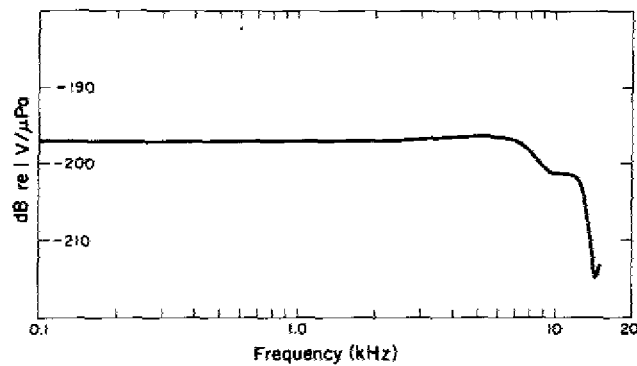


Fig. 20 — Typical free-field voltage sensitivity of an H78A hydrophone without cone adapters

Several measurements were made with an H78A in a set of cone adapters and with a 12-m two-conductor shielded test cable. Figure 21 shows the FFVS. Figure 22 shows the directivity in the xz (vertical) plane at 4, 8, 10, and 12 kHz. The directivity in the xy (horizontal) plane is omnidirectional within ± 1 dB at frequencies up to 5 kHz.

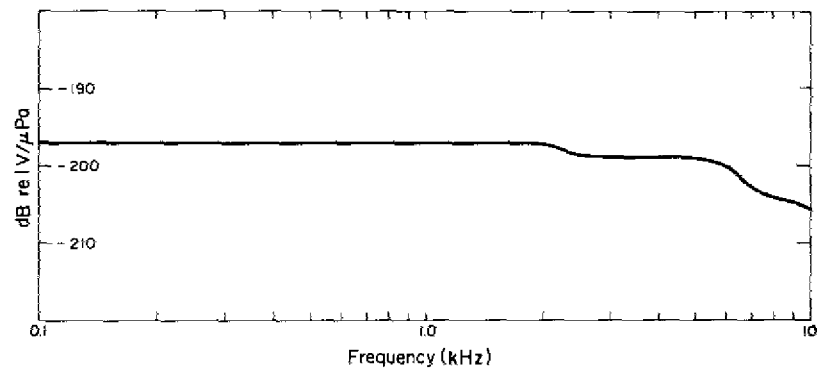
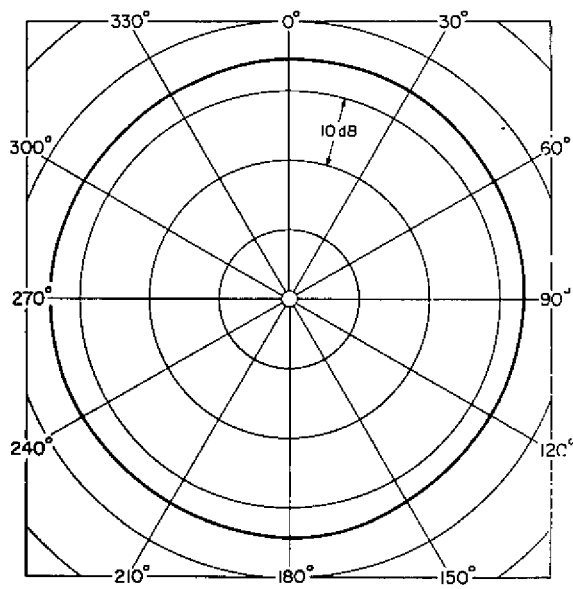
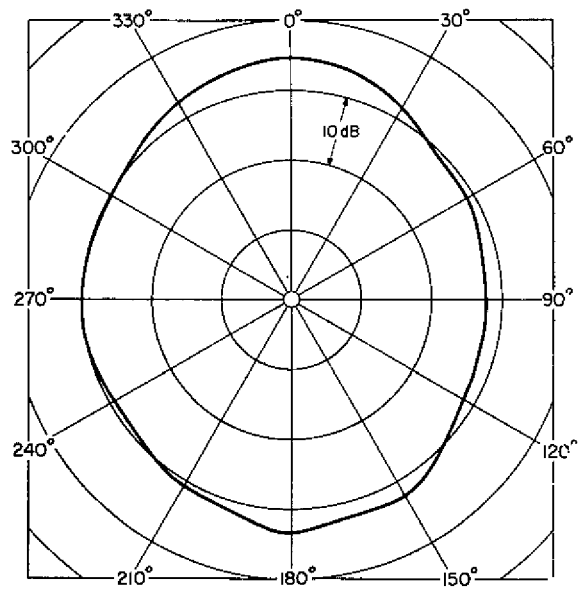


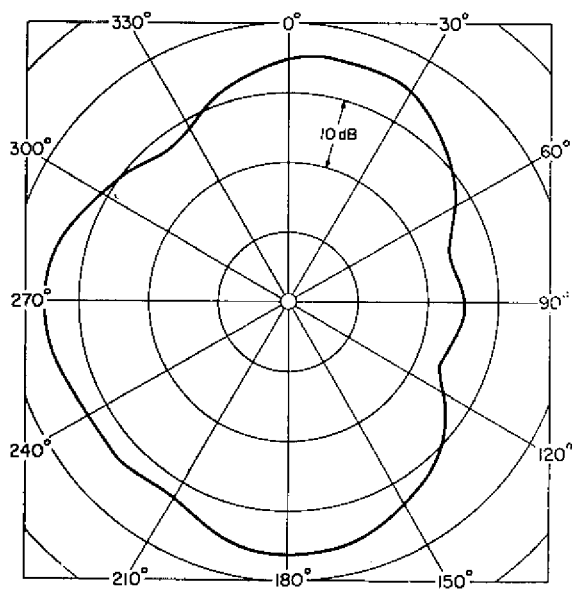
Fig. 21 — Free-field voltage sensitivity of an H78A hydrophone mounted in a set of VEKA I-A cone adapters



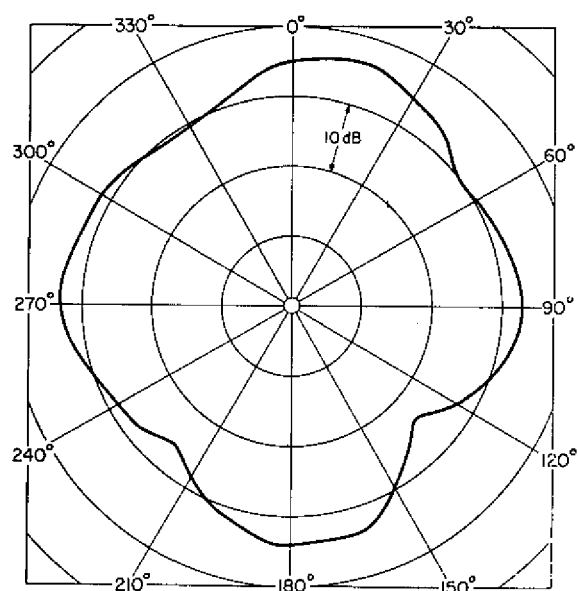
(a) At 4 kHz



(b) At 8 kHz



(c) At 10 kHz



(d) At 12 kHz

Fig. 22 — Typical directivity in the xz plane of an H78A hydrophone mounted in a set of VEKA I-A cone adapters

The typical FFVS of an H78B with a 12-m test cable is shown in Fig. 23. Since the cone adapters are an integral part of the B design, this one curve characterized the response of the hydrophone. Figure 24 shows the typical directivity in the xz plane at 5, 8, 10, and 12 kHz. The directivity in the xy plane is omnidirectional within ± 1 dB at frequencies to 14 kHz. In general the broadband response of the B model is greater than that of the A model, but this is not a requirement for the array.

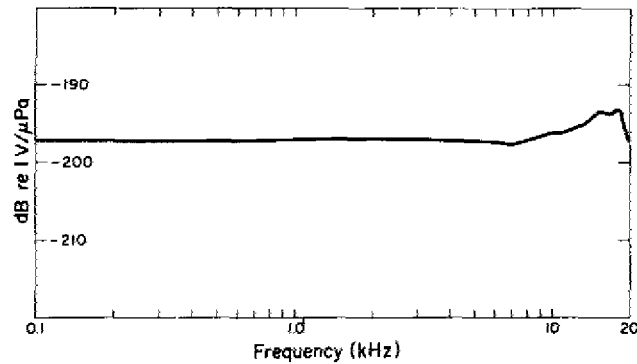


Fig. 23 — Free-field voltage sensitivity of an H78B hydrophone

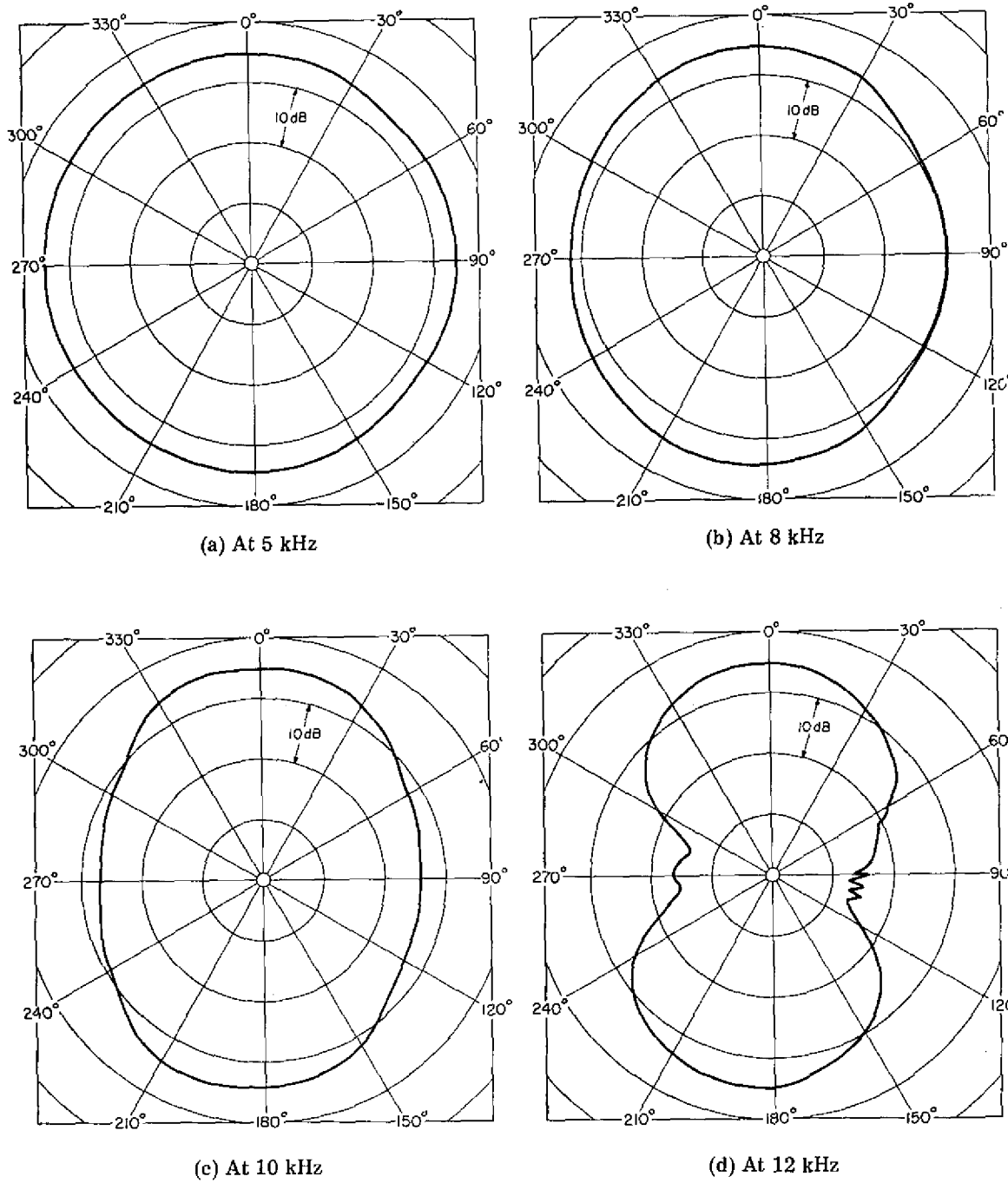


Fig. 24 — Typical directivity in the xz plane of an H78B hydrophone

Figure 25 shows the FFVS of an H78A and an H78B in the VEKA I prototype test cable. The curves show that the VEKA cable itself is the limiting constraint on the response of the array at frequencies above 1 kHz.

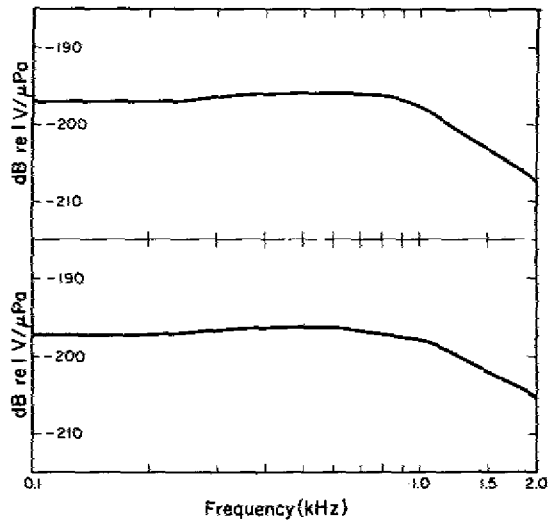


Fig. 25 — Typical free-field voltage sensitivity of (top) an H78A hydrophone in the VEKA I-A prototype cable and (bottom) an H78B hydrophone in the VEKA I-A prototype cable

H78A PREAMPLIFIER SELF-NOISE

Since the FFVS of the H78A is much lower than that of a conventional noise-measuring hydrophone, the self-noise of the preamplifier system can be confusing. This can be clarified by considering the preamplifier circuit as shown in Fig. 26, which is a duplicate of Fig. 7 except that three points in the circuit have been designated for consideration.

At point 1 the preamplifier is in a voltage mode, and a high signal-to-noise ratio exists. With the assumption of a nominal open-circuit crystal sensitivity of -183 dB re 1 V/ μ Pa, and with a gain of 20 dB in A1, the hydrophone sensitivity is -163 dB re 1 V/ μ Pa at point 1. By use of the noise voltage measured at point 1 and the hydrophone sensitivity, the equivalent noise pressure is computed. Figure 27 shows, relative to the guide specification of Fig. 4, the typical equivalent noise pressure of an H78A hydrophone at point 1.

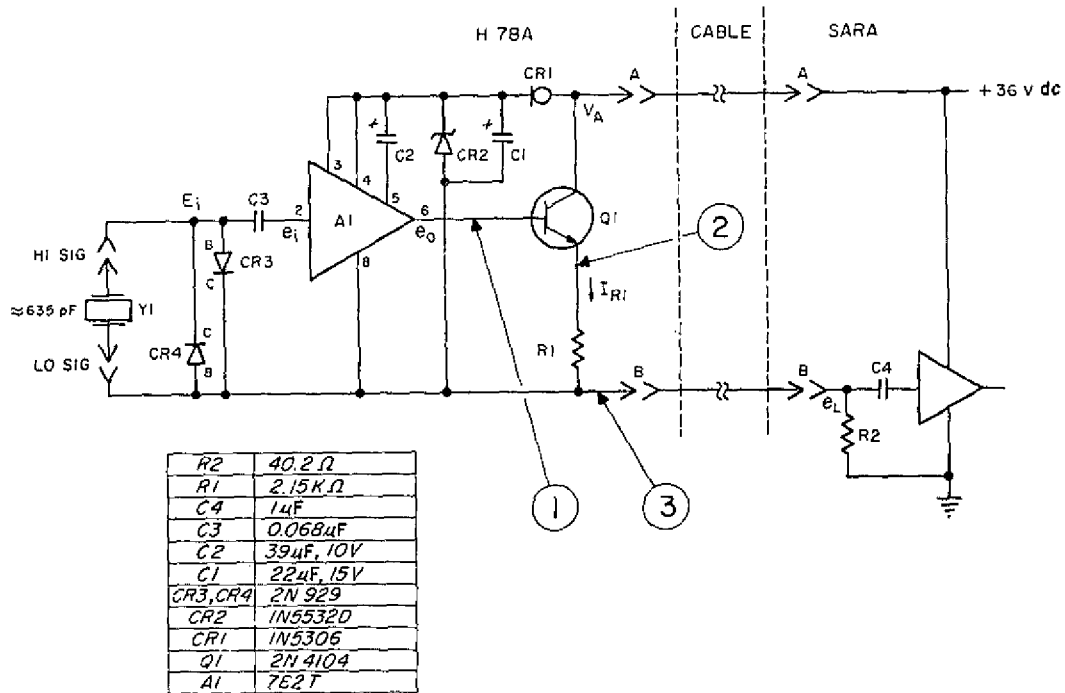


Fig. 26 — Schematic of the H78A preamplifier showing the interface to SARA (one channel)

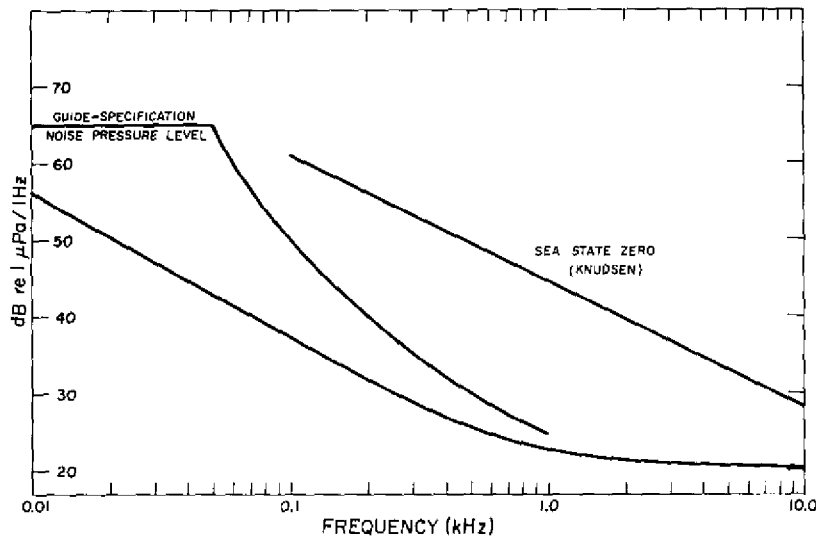


Fig. 27 — Equivalent noise pressure computed from the noise voltage measured at point 1 in Fig. 26

The noise voltage present at point 2 is the same as at point 1. The preamplifier gain is within 0.1 dB of that measured at point 1. The circuit is still in a voltage mode, and no noise has been added by Q1. Therefore the equivalent noise pressure for point 2 is the same as that indicated for point 1.

Point 3 in the circuit is electrically the same as the input of the SARA unit, which is 40.2Ω above ground. When the signal passes through R1, it is changed from a voltage to a current. In reference to point 1 or 2 the signal level is decreased by -34 dB, or in reference to the input of the preamplifier the sensitivity of the hydrophone is decreased by -14 dB. Thus at point 3, or the input to SARA, the hydrophone sensitivity is nominally -197 dB re 1 V/ μ Pa. By use of the noise voltage measured at this point and the sensitivity, the equivalent noise pressure is computed. Figure 28 shows the equivalent noise pressure and shows that the noise starts to increase at about 100 Hz in the current mode and is 10 dB higher than the voltage mode at 1 kHz. The increase in noise is caused by the Johnson-Nyquist noise and the excess noise of R1. The excess noise, sometimes called current noise, exists in addition to the thermal noise of the resistor. The thermal noise dominates at high frequencies, and the excess noise, which has a $1/f$ power spectrum, dominates at low frequencies [13]. Figure 29 shows the individual noise mechanisms in terms of noise voltage and total noise at point 3 in the preamplifier system.

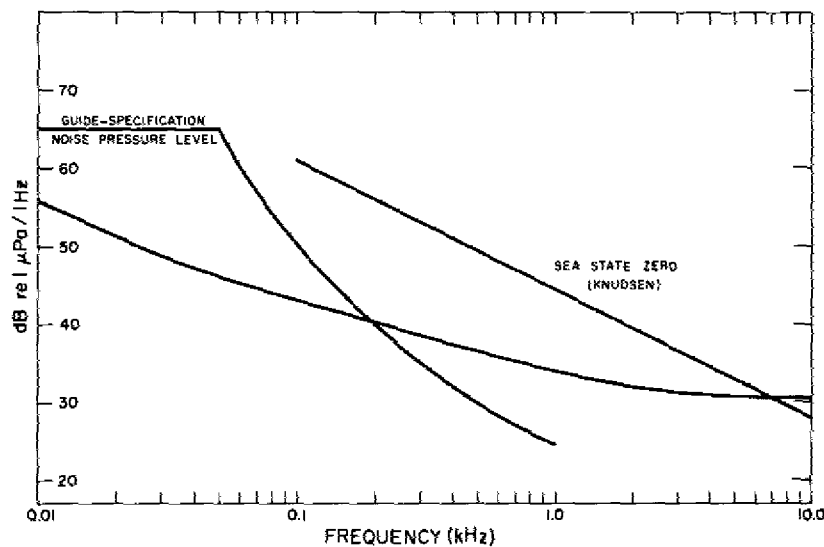


Fig. 28 — Equivalent noise pressure computed from the noise voltage measured at point 3 in Fig. 26

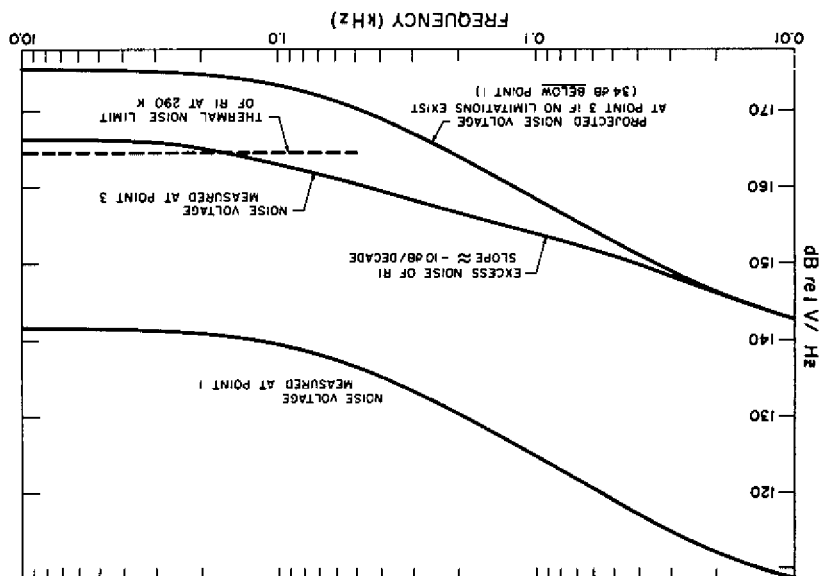


Fig. 29 — Individual noise voltages present at point 3

Operating a preamplifier in a current mode or voltage mode is a compromise between increased self-noise and crosstalk (as will be discussed further in a section on the H78 voltage-mode preamplifier). If the value of R_1 is doubled, the thermal noise would increase 3 dB, which would not be desirable. If the value of R_1 were decreased to half its present value, then the thermal noise limit would be 3 dB lower. However, the dc current required for Q1 would be twice its present value, causing a significant increase in the power required for the array. The value of R_1 was chosen to provide a usable noise floor and to keep the power demand of the array at a minimal level.

DYNAMIC TEST OF PROTOTYPE CABLE AND PROTOTYPE HYDROPHONES

What effect will dynamic loading of the cable have on the hydrophones? Will a hydrophone which slips into the cable (H78B) be more susceptible to cable dynamics than one which uses a cone adapter (H78A) or a sensor cage? These questions were a concern in determining the best hydrophone design for VEKA I. The following information is presented as a basis for choosing the H78A as the most suitable for VEKA.

Figure 30 shows the physical arrangement for the dynamic cable test conducted using a VEKA prototype cable (Appendix E describes the prototype cable) and the H78A and H78B hydrophones. Both hydrophones were rigged within the cable for the test. The driving force was applied to the cable, under tension, by a 1500-W dc motor through a gear reducer with an eccentric crank. The forcing function was approximately sinusoidal at a frequency of 1.4 Hz. A triaxial accelerometer was secured to each hydrophone to determine the acceleration at each hydrophone location. Figure 31 shows one of the hydrophones installed in the test cable. Figure 32 is a close-up of the H78B with the triaxial accelerometer. Figure 33 shows the orientation of the accelerometer and hydrophones with respect to the cable. The accelerometer was attached at the acoustic center of the hydrophones.

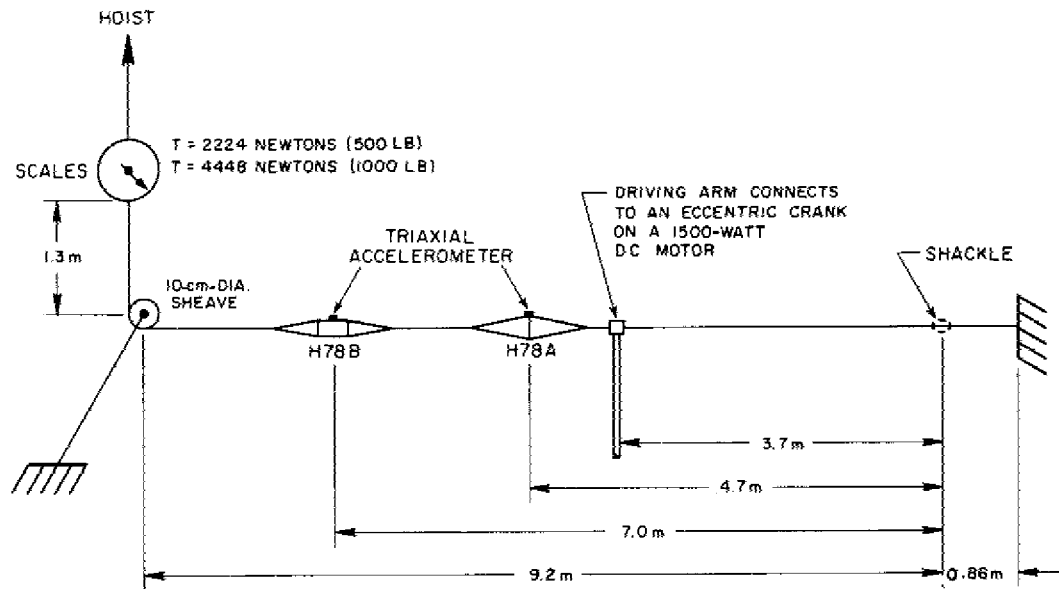


Fig. 30 — Physical arrangement of the VEKA prototype cable and H78 hydrophones for the dynamic test



Fig. 31 — Hydrophone installed in the prototype cable for the dynamic test

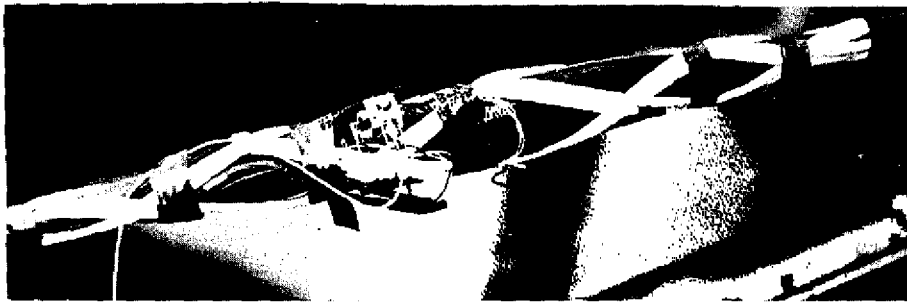


Fig. 32 — H78B hydrophone with a triaxial accelerometer

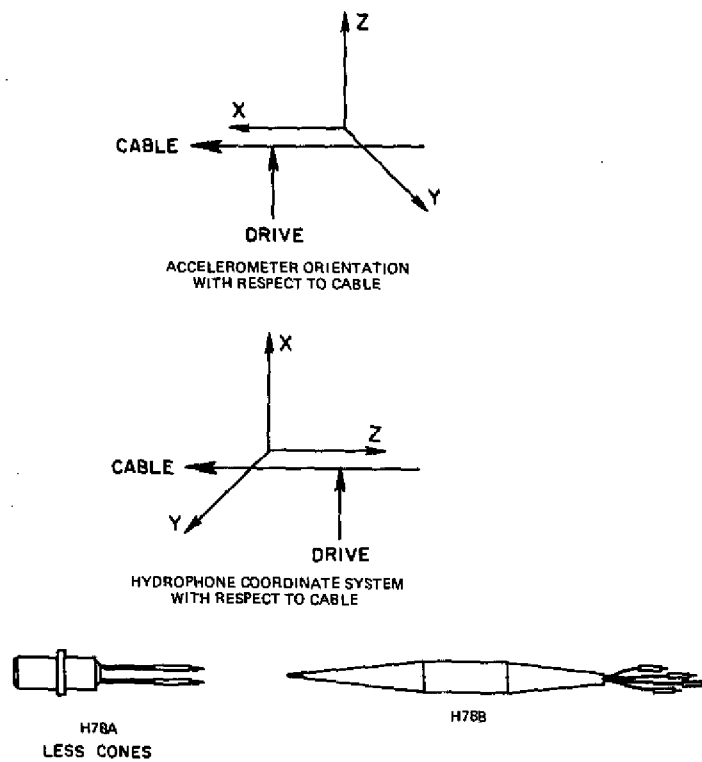


Fig. 33 — Orientation of the hydrophone and the accelerometer

With the cable tensioned to 2224 N and 4448 N respectively, the expected range of cable loading for the array, and with the dc motor driving the cable, the outputs of the hydrophones and the three axes of the accelerometer were analyzed from dc to 20 Hz using a real-time spectrum analyzer and averager. Sixteen spectra were averaged for each output. In the data analysis the hydrophone preamplifier's low-frequency characteristics and the characteristics of the preamplifier used for the accelerometer were accounted for. The tri-axial acceleration present at each hydrophone was determined by the calibration sensitivity of the accelerometer and by the square root of the sum of the squares of the output of each accelerometer axis. Table 4 shows the acceleration data and the test conditions for each hydrophone.

Table 4 — Test Conditions and Acceleration Data for the Dynamic Test of the Prototype Cable and Hydrophones

Hydrophone Type	Driving Frequency (Hz)	Cable Displacement at the Hydrophone (cm)	Accelerometer Outputs (dB re 1 g)			10 log (X ² +Y ² +Z ²)	Hydrophone Output (dBV)	Hydrophone Triaxial Acceleration Sensitivity (dB re 1 V/g)
			X Axis	Y Axis	Z Axis			
Cable Tension = 2224 N								
H78A	1.4	7.4	-14.8	-4.1	1.0	2.3	-25	-27.3
H78B	1.4	3.2	- 9.5	3.2	6.8	8.4	3.2	- 5.2
Cable Tension = 4448 N								
H78A	1.4	7.4	-11.0	0.1	-10.5	0.8	-19.5	-20.3
H78B	1.4	3.2	- 9.6	4.3	5.0	7.8	1.0	- 6.8

Under conditions of cable loading the H78A hydrophone is about 15 to 20 dB less susceptible than the H78B to cable dynamics. The acceleration sensitivity of the H78B should be about equal to or less than that of the H78A. The higher output of the B model is not due to acceleration only but results from cable compressional forces acting directly on the hydrophone, which are subsequently coupled to the sensor element. In the A model the metal rings in the cone adapters isolate the hydrophone from the cable. Therefore, the output of the A model is due to acceleration, and the output of the B model is due to acceleration and pressure.

This is not surprising, as it was generally concluded at the inception of the B model that it would be more subject to cable dynamics. (Also at the inception of the B model, the effects on the cable of possible opens or shorts were analyzed, and these effects are tabulated in Appendix F.) The rationale and concept of the B model are desirable from the standpoint of installation and handling in the VEKA system. However, the dynamic problems associated with it will probably be true of any design in which the hydrophone is not mechanically decoupled or isolated from the cable by a rigid-hoop structure or cage.

HIGH-STRESS EFFECTS ON RADially POLARIZED CAPPED CERAMIC CYLINDERS

For future VEKA considerations and design criterion, several experimental hydrophones were constructed for installation in VEKA I. The H78B, which has been described, is one of the experimental hydrophones; the others were designated H78C, H78D, and H78E. All of the hydrophones have a sensitive element in a radially polarized capped-cylinder configuration. The major difference in each design is in the type of material used for the sensor and the diameter-to-wall-thickness (d/t) ratio. Since the major differences are in the sensor, the mechanical details of these hydrophones will not be discussed here.

Various material types and d/t ratios were used to determine the effects of high stress on the ceramic configuration. As previously stated, there can be considerable variation in the behavior of piezoelectric materials in high-stress applications. Two-dimensional empirical data suggest and data from single-dimension stress measurements [9] strongly suggest that type III material is more resistant than type I to high stress. This scenario represents the general characteristics of the materials but not the characteristics of a specific material from a specific manufacturer. A type I material from one manufacturer can be more stress resistant than a type III material from another manufacturer.

Two-dimensional-stress data obtained from the H78A hydrophone and the experimental hydrophones H78B, H78C, H78D, and H78E are given in Table 5. ΔM_0 is the change in acoustic sensitivity in the flat portion of the response, and ΔK_3 is the percent change in the relative dielectric constant. The table shows that slight changes occur at pressures to 34.5 MPa, but at 69 MPa the sensitivity has decreased about 3 dB in every case and the dielectric constant has decreased by 57% in two of the sensors. The decrease in the dielectric constant represents an increase in the low-frequency cutoff in excess of 1 octave. The hydrophone now has a "new" stress-induced low-frequency cutoff. Also, H78C with a type I ceramic shows no change in dielectric constant at 69 MPa even though the d/t ratio is greater than that of the other type I sensors and one of the type III sensors.

Table 5 clearly illustrates that two-dimensional stresses affect the piezoelectric and dielectric constants of the ceramic. Unfortunately data on the effects of stress on a ceramic cylinder are incomplete, especially in terms of an optimum pressure-stable design. At present, transducer designers rely heavily on past experiences and a cut-and-try approach. This points to a primary problem in high-pressure transducer design. It also points out the need to investigate and quantify changes in sensitivity and dielectric constants to be expected as a result of stresses in capped ceramic cylinders of a specific type and manufacturer.

Table 5 — Two-Dimensional-Stress Data on Ceramic Sensors of Various Diameter-to-Wall-Thickness (d/t) Ratios and From Various Manufacturers

MIL STD 1376 (SHIPS) Material Designation	Manu- facturer	d/t	Used on VEKA Hydro- phone	Pressure = 34.5 MPa		Pressure = 69 MPa	
				Change in Sensitivity ΔM_0 (dB)*	Change in Dielectric Constant ΔK_3 (%)†	ΔM_0 (dB)	ΔK_3 (%)
Type I	Channel Industries Inc.	6.3	H78A and H78B	-1.0	-10.6	-3.0	-38
Type III	Marine Resources Inc.	6.3	H78E	-0.8	0	-2.5	-57
Type I	Vernitron	9.7	H78C	-1.0	0	-3.2	0
Type III	Marine Resources Inc.	9.7	H78D	-1.0	-27	-3.2	-57

* ΔM_0 represents the change in sensitivity in dB referred to the sensitivity at 0.7 MPa.

† ΔK_3 is the percent change in the dielectric constant of the material referred to the dielectric constant at 0.7 MPa.

CALIBRATION OF VEKA I-A HYDROPHONES

Four H78A hydrophones, representative of the manufactured lot of 36, were selected for calibration in the USRD Low-Frequency System K [14]: those with serial numbers 12, 21, 34, and 45. They were calibrated by the comparison method using a USRD type H48 standard reference hydrophone [8]. The frequencies for the calibration ranged from 1 to 1000 Hz, the temperatures were 3 and 23°C, and the pressures were 3.5, 6895, and 3.5 kPa at each temperature over the frequency range. The voltage at the output of an H78A receive amplifier (one SARA channel) was measured open-circuit, and the sensitivity was referred to the input of the receive amplifier, where the hydrophone is terminated in a 40.2- Ω resistor in series with the low side of the output to ground. This makes the sensitivity of the hydrophone independent of the receive amplifier and dependent on the termination resistance. The receive-amplifier characteristics were determined by the insertion method prior to hydrophone calibrations. Table 6 shows the calibration data.

Table 6 — Results of Calibrating USRD Type H78A Hydrophones
in System K (voltage across a 40.2- Ω resistor in series
with the low lead to ground; unbalanced)

Fre- quency (Hz)	Free-Field Voltage Sensitivity (-dB re 1 V/ μ Pa)							
	Serial No. 12		Serial No. 21		Serial No. 34		Serial No. 45	
	3.45 kPa	6895 kPa	3.45 kPa	6895 kPa	3.45 kPa	6895 kPa	3.45 kPa	6895 kPa
Temperature = 3°C								
1	220.5	220.7	221.0	221.0	220.5	220.4	220.7	220.6
2	212.9	213.1	213.4	213.2	212.9	213.1	213.1	213.3
3	209.0	209.2	209.6	209.4	209.2	209.3	209.2	209.4
4	206.5	206.3	207.2	207.0	206.6	206.9	206.9	207.0
5	205.0	205.3	205.5	205.3	205.0	205.3	205.2	205.3
8	201.7	201.9	202.3	202.1	201.9	202.2	201.9	202.2
10	200.8	200.7	201.2	200.9	200.8	201.0	200.9	200.9
20	198.5	198.4	198.8	198.8	198.7	198.8	198.7	198.7
30	197.8	197.7	198.2	198.2	198.1	198.2	198.1	198.2
50	197.4	197.4	197.8	197.8	197.6	197.8	197.7	197.7
80	197.2	197.2	197.6	197.7	197.5	197.6	197.6	197.5
100	197.2	197.1	197.6	197.6	197.6	197.6	197.6	197.5
200	197.1	197.1	197.5	197.5	197.5	197.5	197.6	197.6
500	197.1	196.9	197.5	197.5	197.6	197.5	197.5	197.5
800	197.2	197.6	197.6	197.7	197.5	197.9	197.4	197.9
1000	197.7	197.8	197.9	197.8	197.8	198.0	197.5	198.1
Temperature = 23°C								
1	220.5	220.4	220.7	220.9	220.8	220.8	220.5	220.5
2	212.9	212.6	213.2	213.1	213.3	213.5	212.9	212.9
3	209.2	208.8	209.6	209.1	209.5	209.5	209.1	209.2
4	206.8	206.7	207.3	206.6	207.2	207.0	206.8	206.8
5	205.2	204.9	205.6	204.9	205.5	205.2	205.2	205.3
8	202.1	202.0	202.6	201.8	202.4	202.0	202.1	202.3
10	200.8	200.8	201.4	200.8	201.3	200.9	201.1	201.2
20	198.5	198.4	199.2	198.8	199.0	198.9	198.8	198.8
30	197.8	197.8	198.4	198.7	198.3	198.2	198.2	198.2
50	197.3	197.4	197.9	197.8	197.9	197.8	197.7	197.7
80	197.2	197.3	197.7	197.7	197.7	197.7	197.5	197.6
100	197.1	197.2	197.7	197.6	197.6	197.6	197.5	197.5
200	197.2	197.2	197.5	197.5	197.5	197.5	197.4	197.5
500	197.0	197.0	197.4	197.3	197.5	197.2	197.3	197.2
800	197.2	197.5	197.7	197.8	197.7	197.7	197.6	197.8
1000	197.4	197.6	197.9	197.9	197.8	197.8	197.8	197.8

From the four hydrophones calibrated in System K, those with serial numbers 12 and 21 were selected for calibration in the USRD System J [15,16] to characterize the effects of high hydrostatic pressure. The results are shown in Table 7.

Table 7 — Results of Calibrating USRD Type H78A Hydrophones in System J (unbalanced; temperature = 5°C)

Frequency (Hz)	Electroacoustic Characteristics							
	0.345 MPa		13.8 MPa	27.6 MPa	41.4 MPa	55.1 MPa	68.9 MPa	
	FFVS*	Phase†	FFVS*	FFVS*	FFVS*	FFVS*	FFVS*	Phase†
Serial No. 12								
5	204.5	— ‡	204.8	205.7	207.2	209.1	210.6	— ‡
7	202.3	— ‡	202.5	203.4	205.1	206.8	208.4	— ‡
10	200.4	228.6	200.6	201.3	202.7	204.0	205.6	245.1
11	— ‡	225.7	— ‡	— ‡	— ‡	— ‡	— ‡	241.3
12	— ‡	222.6	— ‡	— ‡	— ‡	— ‡	— ‡	240.7
13	— ‡	222.3	— ‡	— ‡	— ‡	— ‡	— ‡	236.7
14	— ‡	220.4	— ‡	— ‡	— ‡	— ‡	— ‡	236.0
15	198.9	218.6	199.1	199.8	201.0	202.3	203.7	235.5
20	198.2	209.9	198.4	199.0	200.0	201.7	202.3	227.9
50	197.4	193.2	197.4	198.0	198.8	199.7	200.6	198.9
100	197.2	186.9	197.4	197.9	198.6	199.4	200.2	190.1
200	197.1	183.3	197.3	197.7	198.5	199.2	200.0	185.4
500	197.2	179.7	197.4	197.8	198.5	199.3	200.1	180.2
800	197.5	178.1	197.4	197.9	198.6	199.3	200.2	179.3
1000	197.4	176.7	197.6	197.9	198.6	199.4	200.2	177.3
1200	197.6	175.8	197.7	198.1	199.0	199.4	200.3	175.5
Serial No. 21								
5	204.9	— ‡	205.2	206.2	207.8	209.7	211.1	— ‡
7	202.7	— ‡	203.0	203.9	205.3	207.0	208.5	— ‡
10	200.9	227.7	201.1	201.8	203.3	204.8	206.2	240.2
11	— ‡	224.8	— ‡	— ‡	— ‡	— ‡	— ‡	237.4
12	— ‡	221.1	— ‡	— ‡	— ‡	— ‡	— ‡	237.4
13	— ‡	221.4	— ‡	— ‡	— ‡	— ‡	— ‡	234.2
14	— ‡	219.5	— ‡	— ‡	— ‡	— ‡	— ‡	232.0
15	199.4	217.6	199.6	200.2	201.5	202.7	204.1	230.2
20	198.7	209.2	198.9	199.5	200.6	201.7	202.9	219.4
50	197.8	192.8	197.9	198.5	199.3	200.1	201.2	197.8
100	197.7	186.5	197.8	198.3	199.1	199.9	200.8	189.4
200	197.6	183.2	197.8	198.2	199.0	199.8	200.6	184.9
500	197.7	179.8	197.8	198.3	199.1	199.9	200.7	190.7
800	197.9	179.6	197.9	198.3	199.1	199.9	200.7	179.4
1000	197.8	176.7	198.0	198.4	199.1	199.9	200.8	177.8
1200	198.0	175.1	198.3	198.7	199.5	200.0	200.9	175.8

*Free-field voltage sensitivity (FFVS) in \sim dB re 1 V/ μ Pa; voltage across a 40.2- Ω resistor in series with the low lead to ground.

†Acoustical phase in positive degrees. The reference hydrophone was USRD type H48, serial No. 1.

‡No measurements required.

After evaluation in System J the H78A hydrophone with serial number 21 was selected as a comparison standard to calibrate the remaining H78A hydrophones in a USRD type G40 calibrator [17]. Calibrator measurements indicated that the sensitivity of all of the H78A's were within ± 0.4 dB of the standard.

After the preceding calibrations were completed, the hydrophones were installed in the array cable by NORDA personnel. The entire array was then shipped to the USRD Leesburg Facility for final calibration. Figure 34 shows a typical response curve for an H78A hydrophone in the array. Calibration data for each hydrophone in the array are given in USRD Calibration Report 4467.

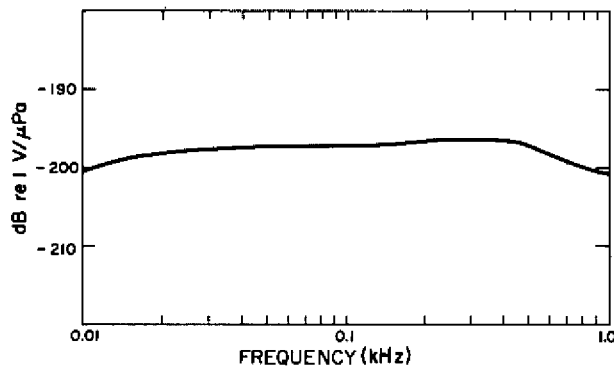


Fig. 34 — Typical free-field voltage sensitivity of a VEKA I-A hydrophone

USRD TYPE H78D HYDROPHONE

During the development of the VEKA I hydrophones USRD was tasked by NORDA to develop a small, inexpensive hydrophone for future arrays. The hydrophone population of future arrays is expected to double or quadruple the present array population; thus a reduction in cost is very desirable. A small hydrophone obviously presents a smaller bulge in the cable and is less vulnerable to damage during deployment of the array. It is desired, however, that the capabilities of the hydrophone be compromised as little as possible, even though size and cost reductions will require some compromises.

Description

Figure 35 is a sectional view of the hydrophone designated as USRD type H78D. The hydrophone boot is an electrical-grade butyl rubber (USRD compound 70821). In the end of the boot is an oil-fill hole; the metal port is vulcanized and bonded in place. Four rubber tips are molded integral with the boot and allow the hydrophone to be snapped into a cone adapter. The crystal assembly is similar to that of an H78A but smaller, with aluminum oxide caps on both ends. The crystal material is a type III ceramic. A current-mode pre-amplifier identical to the H78A circuit is enclosed within the sensor assembly. A castable RHO-c elastomer potting forms the cable gland and permanently seals the hydrophone boot.

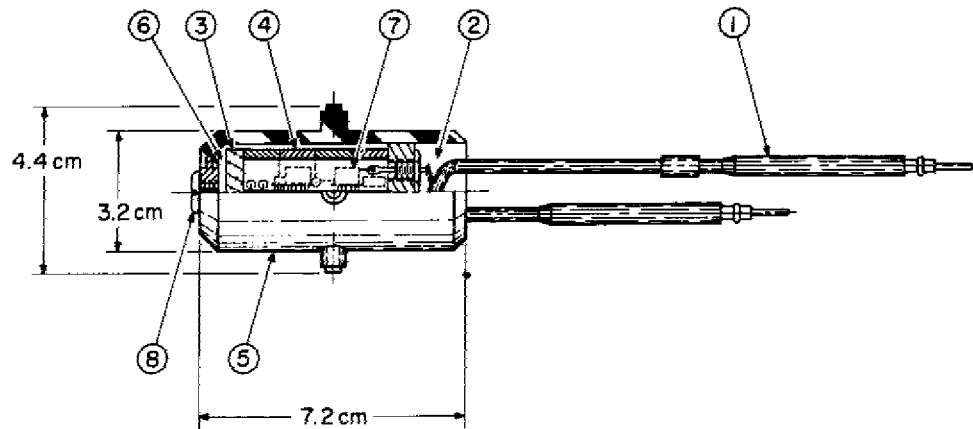


Fig. 35 — Sectional view of a USRD type H78D hydrophone: (1) connector, (2) potted cable assembly, (3) aluminum oxide end cap, (4) ceramic sensor, (5) butyl rubber boot with integral mounts, (6) castor oil, (7) preamplifier, and (8) oil-fill screw

It is assumed that VEKA I will provide all the data necessary to allow a sealed non-reenterable hydrophone in future arrays. Therefore the H78D is not reenterable, which eliminates the major machine parts with O-ring surfaces as found in the A model. The aluminum oxide caps can be obtained from the manufacturer at a moderate cost. A large-quantity purchase would offer significant cost reduction.

In comparison with the H78A model the H78D model is 46% smaller by volume, 17% smaller in diameter, and 21% shorter in length. A significant reduction in size has been achieved. The diameter-to-wall-thickness ratio of the crystal has been increased, which makes the hydrophone more susceptible to high stress, but the material was changed to the more stress-resistant type III ceramic.

Four radially polarized rings with a 2.22-cm o.d., a 1.76-cm i.d., and a 0.953-cm length are bonded together and electrically wired in series to form the sensor assembly. The theoretical sensitivity of a single crystal is -196.4 dB re 1 V/ μ Pa; for four crystals in series $M_0 = -184$ dB. The capacitance of a single element is 2300 pF and of four elements in series is 575 pF. The sensitivity and capacitance compare favorably with those of the H78A, the sensitivity being 1.5 dB less and the capacitance 4-1/2% less. This makes the noise floor about 2 dB higher than that of the H78A.

Table 8 shows the calibration data of the H78D hydrophones having serial numbers 1 and 2. Measurements were made in the USRD System J.

Table 8 — Results of Calibrating USRD Type H78D Hydrophones in System J
(Temperature = 5°C)

Frequency (Hz)	Free-Field Voltage Sensitivity (-dB re 1 V/ μ Pa)					
	Serial No. 1*			Serial No. 2*		
	0.689 MPa [†]	34.5 MPa	68.9 MPa	0.689 MPa [†]	34.5 MPa	68.9 MPa
5	203.4	206.1	210.8	203.6	205.1	211.7
7	201.5	204.0	208.7	201.6	203.5	209.8
10	199.6	201.9	206.9	199.4	201.3	207.6
20	197.5	199.1	203.2	197.2	198.7	203.3
50	196.5	197.7	200.5	196.3	197.4	200.3
100	196.3	197.4	199.9	196.1	197.2	199.5
200	196.3	197.3	199.9	196.0	197.1	199.7
500	196.4	197.6	199.9	196.2	197.2	199.7
800	196.5	197.6	199.9	196.3	197.3	199.7
1000	196.5	197.6	199.9	196.3	197.3	199.7
1200	196.5	197.6	199.9	196.3	197.3	199.7

* Voltage across a 40.2- Ω resistor in series with the low lead to ground.

[†] 0.689 MPa after 68.9 MPa repeats within ± 0.2 dB.

Cone Adapters

The cone adapters for the D model represent a significant cost reduction and are much simpler than previous models. Figure 36 shows a D-model hydrophone in its cone adapter. A small section of schedule-40 PVC pipe 3.81 cm (1-1/2 in.) in diameter serves as the radial strength member and hydrophone mount. The rubber cones snap into a groove in the pipe as shown, or they can be designed to slip over the outside of the pipe and clamp in place with a band. Both designs were evaluated, and the latter is the least expensive, because it requires less machining. The hydrophone slips into the pipe and the four rubber tips (Fig. 36) are engaged by the four holes. Other holes can be put into the wall of the pipe to aid in flooding the assembly.

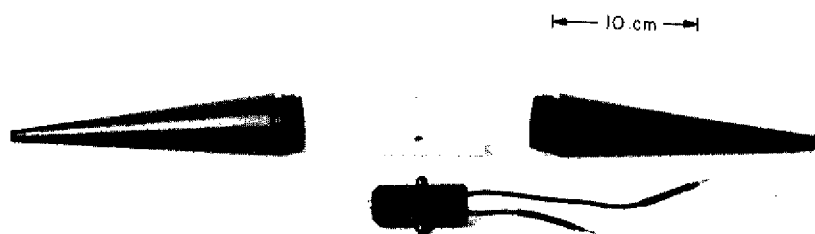


Fig. 36 — H78D hydrophone with cone adapters

Comparison of an assembled set of the D-model cone adapters with the MABS adapters and VEKA I-A adapters is shown in Table 9. Mass and size have been significantly reduced in each new generation. Obviously the acoustical performance has been enhanced with each new generation, as there are fewer extraneous materials in the sound field.

Table 9 — Comparison of MABS, VEKA I-A, and D-Model
Cone Adapter Sets

Adapter Set	Mass (kg)	Length (cm)	Diameter (cm)
MABS	≈3.8	≈124	10.2
VEKA I	≈1.6	≈ 81	7.6
D Model	≈0.6	51	5.0

H78 VOLTAGE-MODE PREAMPLIFIER

The original design for the H78 hydrophone preamplifier was a voltage-mode device. The final design was a current-mode circuit. The difference is that in a voltage-mode preamplifier the output signal is in the form of a varying voltage whereas in a current-mode device the output signal is a controlled ac current. Either design can use a two-wire cable, but a current-mode preamplifier can be terminated in a very low impedance whereas the voltage-mode device must be terminated in a high impedance. Cable resistance will not affect the output of a current-mode preamplifier, but it will attenuate the output of a voltage-mode device (cable capacitance affects both outputs). Self-noise is generally lower in a voltage-mode design than in a current-mode design.

It was felt that crosstalk at the end of the VEKA cable would be excessive if the cable were terminated in high-impedance loads. Hence a current-mode preamplifier was ultimately used in the VEKA project. A simplified version of the abandoned voltage-mode preamplifier is shown in Fig. 37. In this configuration, supply current originates at the load supply E_{dc} . It is regulated as shown to a constant value, I_{dc} . This current, which is unaffected by cable length, reaches the preamplifier and divides itself among amplifier A1, line driver A2, and zener diode CR1. Zener CR1 establishes the dc supply voltage V_{cc} for the preamplifier. The audio output signal is coupled by C1 and C2 to the load. The current regulator producing I_{dc} appears as an open circuit to this audio signal. The signal is loaded, however, by R1 and R2. To avoid significant losses in the cable, R2 must be much greater than the cable resistance. Resistor R1 must also be large to avoid excessive loading of A2.

One experimental voltage-mode preamplifier was used in the VEKA array (H78C). It was a USRD type-H80 preamplifier which differs somewhat from the original VEKA design described here. It served to compare voltage and current modes of operation in the array.

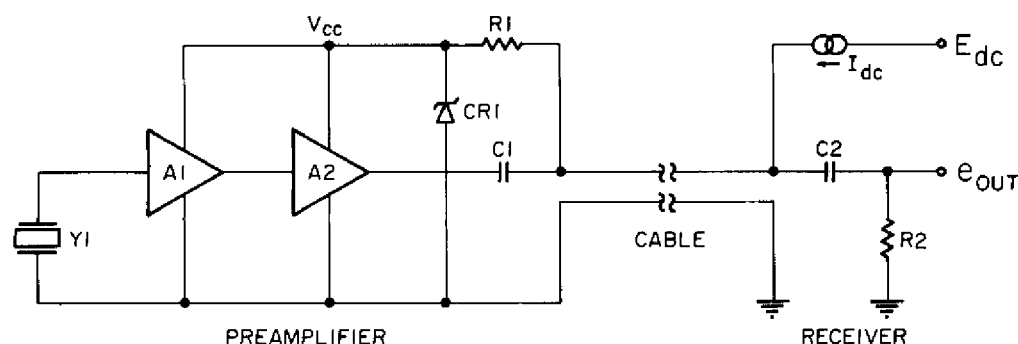


Fig. 37 — Simplified diagram of the voltage-mode preamplifier, later abandoned

CONCLUSION

A major objective of VEKA I-A is to provide a wide-aperture system with increased reliability, versatility, and performance. The approach was to specifically design hydrophones that are made an integral part of the cable during fabrication. The VEKA with the H78 hydrophones and the SARA are expected to provide important information for further development of multipurpose, free-flooded, distributed sensor systems with Kevlar strength members.

ACKNOWLEDGMENTS

The authors thank Mr. M. D. Jevnager of the USRD Development Section for his engineering skill in the design of the cone adapter mold and his workmanship in assembling the hydrophones. Thanks are due to Mr. Paul Brooks of the USRD Machine Shop for his precise machine work, his cooperative spirit during changing situations, and his prompt completion of the molds for the project and parts for the developmental hydrophones. Mr. J. C. Mathis of the USRD Services Section is commended for the cone adapters he molded. Thanks are due also to Mr. G. M. Norton of the USRD Electronics Branch for the design layout and fabrication of SARA.

REFERENCES

1. R.C. Swenson, "The Cable Development Program for Suspended Sensor Applications," NUSC Technical Report 4915, 22 Sept. 1975.
2. D.A. Milburn and R.C. Swenson, "VEKA I-A: Design and Fabrication," a NORDA report to be published.
3. C.C. Sims and T.A. Henriquez, "Reciprocity Calibration of a Standard Hydrophone at 16,000 psi," *J. Acous. Soc. Am.* 36, 1704-1707 (1964).

4. T.A. Henriquez and L.E. Ivey, "Standard Hydrophone for the Infrasonic and Audio-Frequency Range at Hydrostatic Pressure to 10,000 psig," *J. Acous. Soc. Am.* **47**, 276-280 (1970).
5. T.A. Henriquez, "Calibration at High Pressure of Piezoelectric Elements for Deep-Submergence Hydrophones," *J. Acous. Soc. Am.* **46**, 1251-1253 (1969).
6. A.C. Tims, "Hydrophone Preamplifier Optimization-Prediction of Hydrophone Self-Noise by a Noise Model," NRL Report 8180, 17 Mar. 1978.
7. MIL-STD 1376 (SHIPS), "Piezoelectric Ceramic for Sonar Transducers," 21 Dec. 1970.
8. L.E. Ivey, "High-Pressure Piezoelectric Ceramic Hydrophone for Infrasonic and Audio Frequencies USRD Type H48," NRL Report 7260, 15 Mar. 1971.
9. S.W. Meeks and R.W. Timme, "Effects of One-Dimensional Stress on Piezoelectric Ceramics," *J. Applied Phys.* **46**, 4334-4338 (Oct. 1975).
10. R.A. Langevin, "The Electro-Acoustic Sensitivity of Cylindrical Ceramic Tubes," *J. Acous. Soc. Am.* **26**, 421-427 (1954).
11. R.T. Winnicki and S.E. Auyer, "Geometric Factors Affecting Hydrophone Performance," *J. Acous. Soc. Am.* **61**, 876-881 (Mar. 1977).
12. C.K. Brown and A. C. Tims, "Hydrophone Preamplifier Optimization-Hybrid Micro-electronics for Low-Noise Hydrophones," NRL Report 8218, 15 June 1978.
13. C.C. Motchenbacher and F.C. Fitchen, *Low-Noise Electronic Design*, Wiley, New York, 1973, pp 171-179.
14. H.J. Hebert and L.P. Browder, "Underwater Sound Transducer Calibration System for the 0.3- to 200-Hz Frequency Range at Hydrostatic Pressure to 6.89 MPa," NRL Report 7502, 20 Oct. 1972.
15. L.G. Beatty and J.F. Prandoni, "Underwater Sound Transducer Calibration Facility for the 10- to 4000-Hz Frequency Range at Hydrostatic Pressure to 10,000 psig," NRL Report 6965, 15 Aug. 1969 (AD-693,091).
16. I.D. Groves, Jr., and T. A. Henriquez, "Electroacoustic Transducers for a 10,000-psig Underwater Sound Transducer Calibration Facility for the Frequency Range 10 to 4000 Hz," NRL Report 6967, 15 Aug. 1969.
17. G.D. Hugus, III and I.D. Groves, Jr., "Hydrophone Calibrator for Shipboard Use," *J. Acous. Soc. Am.* **56**, 70-74 (July 1974).

Appendix A

CALCULATIONS OF SENSITIVITY AND CAPACITANCE OF VARIOUS PIEZOELECTRIC SENSORS

DEFINITION OF TERMS

Symbols to be used in this appendix are defined as follows:

- M_0 = free-field voltage sensitivity in dB re 1 V/ μ Pa,
 e = open-circuit voltage,
 P_0 = incident sound pressure,
 g_{33}, g_{31} = piezoelectric voltage constants in V·m/N (Table A1),
 K_{33}^T = relative dielectric constant (Table A1),
 ϵ_0 = permittivity of free space,
 C = capacitance,
 t = thickness between electrode surfaces,
 a = inner radius,
 b = outer radius,
 ρ = a/b = ratio of the inner radius to the outer radius,
 A = cross-sectional area of the electrode surface,
 l = length of the cylinder.

Table A1 — Piezoelectric and Dielectric Constants for Several Materials

Material	g_{31} (10^{-3} V·m/N)	g_{31} (10^{-3} V·m/N)	K_{33}^T
Lithium Sulfate	—	148	10.3
Lead Metaniobate	— 4.5	36.0	250
Type I	-10.7	24.5	1300
Type II	-11.2	24.5	1750
Type III	— 9.1	24.4	1000

DISK OR PLATE

Lithium Sulphate

The free-field voltage sensitivity of a lithium sulphate disk of thickness t , when the sound pressure is impinging on all surfaces and the size is small in comparison with a wavelength, is

$$\frac{e}{P_0} = g_{33} t, \quad (\text{A1})$$

If $t = 3.18 \times 10^{-3}$ m (1/8 in.), then

$$\frac{e}{P_0} = 0.148 (3.18 \times 10^{-3}) \text{ V} \cdot \text{m}^2/\text{N},$$

and if $P_0 = 1 \mu\text{Pa}$ (10^{-6} N/m²), then

$$e = 4.7 \times 10^{-10} \text{ V}/\mu\text{Pa},$$

so that $M_0 = 20 \log 4.7 \times 10^{-10} = -186.6$ dB re 1 V/ μPa . If the crystal has a radius of 1.27×10^{-2} m (1/2 in.), then the capacitance is

$$C = \epsilon_{33} A/t = 8.85 \times 10^{-12} K_{33}^T A/t, \quad (\text{A2})$$

so that

$$C = 14.6 \text{ pF}.$$

Lead Metaniobate

For a lead metaniobate disk the sensitivity is

$$\frac{e}{P_0} = (g_{33} + 2g_{31})t, \quad (\text{A3})$$

and if $t = 6.35 \times 10^{-3}$ m (1/4 in.) and $P_0 = 1 \mu\text{Pa}$, then

$$e = 1.71 \times 10^{-10} \text{ V}/\mu\text{Pa},$$

so that

$$M_0 = -195 \text{ dB re } 1 \text{ V}/\mu\text{Pa}.$$

The capacitance is given by equation A2. If the disk has a radius of 1.27×10^{-2} m, then

$$C = 177 \text{ pF}.$$

CAPPED CYLINDER

The sensitivity and capacitance of a specific radially capped cylinder are presented in the main text of this report; therefore only the equations are presented here (equations 1 and 2 of the main text):

$$\frac{e}{P_0} = b \left[g_{33} \left(\frac{1-\rho}{1+\rho} \right) + g_{31} \left(\frac{2+\rho}{1+\rho} \right) \right] \quad (\text{A4})$$

and

$$C = \frac{2\pi \epsilon_{33} \ell}{\ln(b/a)}. \quad (\text{A5})$$

SPHERE

The free-field voltage sensitivity of a ceramic sphere has been derived by Anan'eva*:

$$\frac{e}{P_0} = \frac{b}{\rho^2 + \rho + 1} \left(\frac{\rho^2 + \rho - 2}{2} g_{33} - \frac{\rho^2 + \rho + 4}{2} g_{31} \right). \quad (\text{A6})$$

For a type I ceramic of outside radius $b = 1.27 \times 10^{-2}$ m and inside radius $a = 0.95 \times 10^{-2}$ m

$$\frac{e}{P_0} = 1.197 \times 10^{-10} \text{ V}/\mu\text{Pa}$$

and if $P_0 = 1 \mu\text{Pa}$, then

$$M_0 = -198.4 \text{ dB re } 1 \text{ V}/\mu\text{Pa}.$$

The capacitance of a sphere is given by

$$C = \frac{4\pi \epsilon_{33} ab}{b-a} = \frac{4\pi \epsilon_0 K_{33}^T ab}{b-a}, \quad (\text{A7})$$

so that

$$C = 5508 \text{ pF}.$$

*A. A. Anan'eva, *Ceramic Acoustic Detector*, Consultants Bureau, New York, 1965, p 56.

Appendix B

H78A REPRODUCIBILITY AND MATCHING

In a group of hydrophones constructed to identical specifications, any variability in sensitivity can usually be attributed to the sensor. Careful design and construction of the preamplifier can make the ceramic element the dominant factor. Differences in the piezo-electric constants g_{33} and g_{31} of the ceramic material and, to a lesser extent, the dielectric constant are the major causes of variability. Unfortunately slight differences in the ceramic composition and production techniques can cause the characteristics of ceramics to differ not only from one manufacturer to another but also from one batch to another by the same manufacturer.* Even crystals pressed from the same batch but fired in different furnaces can show significant variations.

Not explicitly stated in the VEKA hydrophone specifications, but certainly implied by the nature of the array, is that the sensitivity and overall response of the hydrophones be identical within practical limits. To accomplish this, the first step is to obtain the required crystals from one manufacturer and from the same batch. Dimensional tolerances can be held close to increase uniformity, especially in the capacitance. In lieu of actual calibration of each sensor element and using a sensitivity-capacitance product as a figure of merit, normalizing the capacitance between each sensor stack is the next best approach.

Thirty-six H78A hydrophones were required for the program (32 in the array with four spares), or 144 individual crystal elements. To fill this need, 160 radially polarized cylinders of type I ceramic were obtained from Channel Industries, Santa Barbara, California. Eighty elements polarized positive on the inside electrode and 80 polarized negative were purchased.

Each cylinder was assigned a serial number; then the capacitance of each was measured using a General Radio 1615-A capacitance bridge, and the values were recorded. Of the 80 positive elements the mean capacitance \bar{C} was 2355 pF with a standard deviation σ of 37 pF. For the 80 negative elements \bar{C} was 2349 pF with $\sigma = 40$ pF. The capacitances of all the elements were within $\pm 3\sigma$. The standard deviation was calculated using the formula

$$\sigma = \left[\frac{\sum_{i=1}^N (C_i - \bar{C})^2}{N-1} \right]^{1/2}, \quad (\text{B1})$$

where C_i is the individual crystal capacitance, \bar{C} is the mean crystal capacitance, and N is the number of elements.

*R.W. Timme, "Low Electrical Field Characteristics of Piezoelectric Ceramic Rings," NRL Report 7528, 5 Jan. 1973 (AD-907,068L).

After the capacitance was measured, the elements were arranged or ranked in two rows according to each capacitance value, with the 80 negatively polarized elements in one row and the 80 positive elements in another. Since 144 elements were required to complete the 36 hydrophones, the four extreme minimum capacitance elements and the four extreme maximum capacitance elements were removed from each row, leaving the required 144 elements. The elements for each sensor assembly were then selected by taking two minimum capacitance negatively polarized elements and combining them with two maximum capacitance positively polarized elements as shown in Fig. B1. The selection process was repeated until all elements were dedicated to a specific assembly.

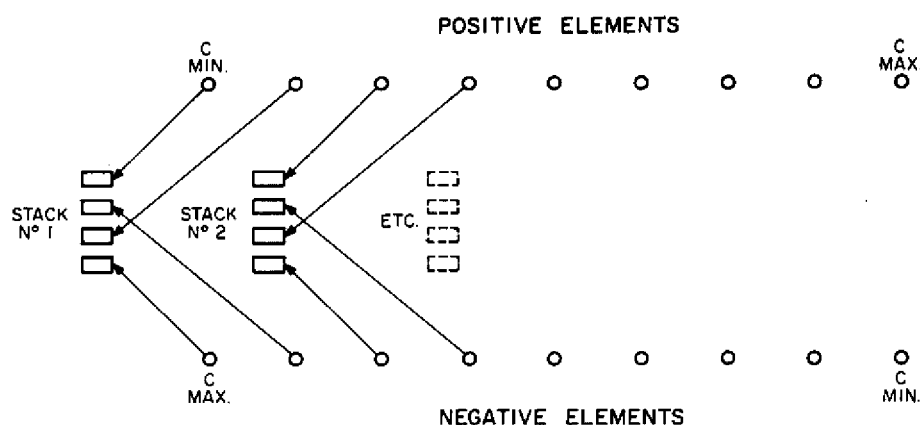


Fig. B1 — Crystal selection process

With use of the measured capacitance of each element and the series capacitance formula, the expected capacitance for the 36 sensor assemblies was calculated. The calculated mean assembly capacitance was 588 pF with $\sigma = 1.0$ pF. The calculated capacitance range was from 587 to 589 pF. The small σ indicates that the method of selecting and combining the elements effectively normalized the capacitance between sensor assemblies.

After the crystal elements were bonded together and appropriately wired, the measured mean capacitance of the 36 assemblies was 631 pF with $\sigma = 6$ pF. The measured values were higher than the calculated values because of stray capacitance and fringing between the assembled elements and because of the addition of electrode wires. All the assembled sensors were within 2σ of the measured mean capacitance, with the measured capacitance ranging from 622 to 641 pF.

To further increase uniformity of the H78A hydrophones, care was taken in their assembly to insure that all of the hydrophones were of the same electrical phase. This was done by checking to see that the polarity marks indicated by the manufacturer on the crystals were true and by carefully observing the marks during sensor assembly. The assembled sensors were then "squeeze" tested, and the direction of charge polarity was observed on an electrometer. Observation of the electrical phase at the output of the hydrophones, during calibration in the G40 calibrator, served as final test of uniformity.

Appendix C

H78B CURRENT-MODE PREAMPLIFIER

The preamplifier used in the H78B hydrophone is shown schematically in Fig. C1. This circuit is identical to that of the H78A preamplifier (Fig. 7) except for the addition of a special calibration circuit consisting of components IS1, R2, R3, and R4. Only the calibration circuit will be explained here, since the remaining circuitry was described in the H78A section of the main body of this report.

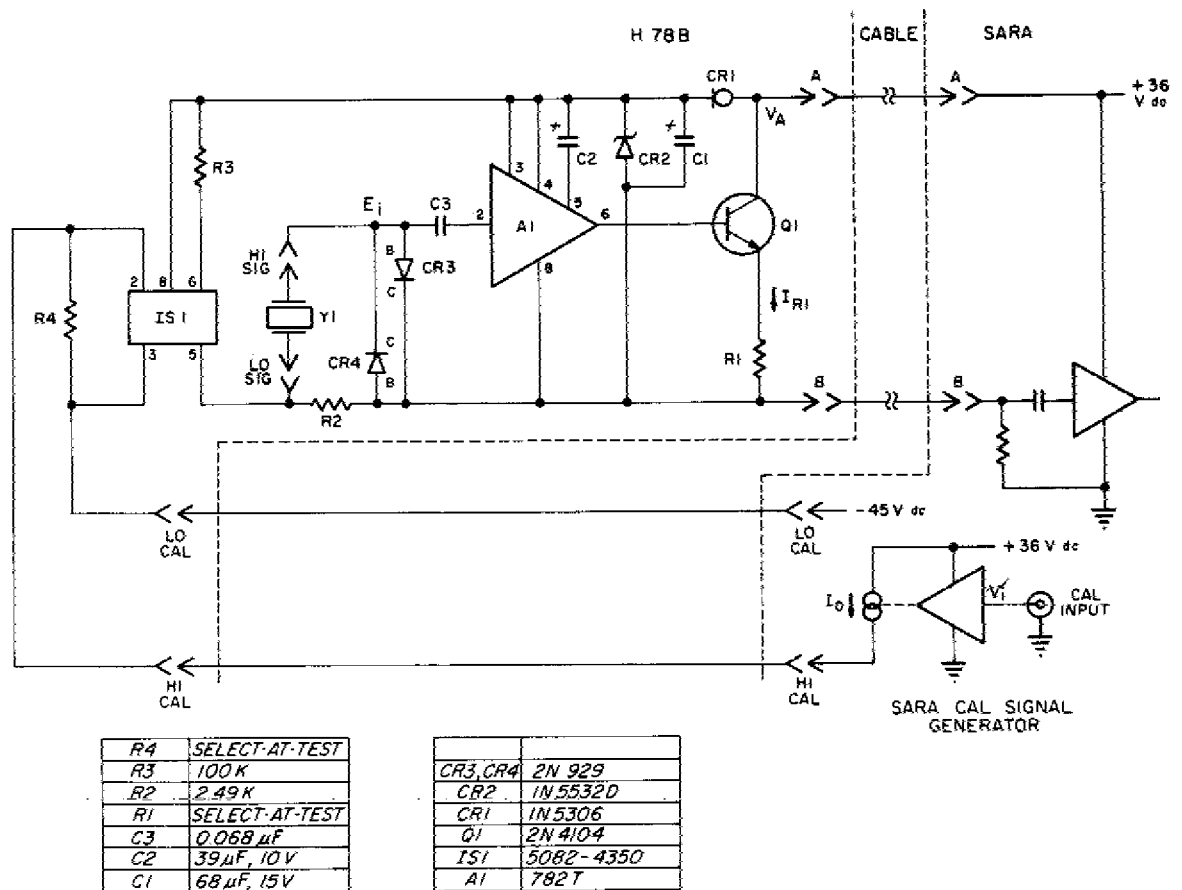


Fig. C1 — Schematic of the H78B hydrophone preamplifier showing the interface to SARA (one channel)

Component IS1 is an optoisolator. Pins 2 and 3 are connected to the anode and cathode respectively of an internal light-emitting diode (LED). Optical coupling within IS1 enables current flowing into the device at pin 2 to be proportionally transferred to output pins 5 and 6 while maintaining electrical isolation between input and output.

The SARA chassis contains a special circuit for generating a calibration signal (Fig. 19). This signal generator delivers a controlled current I_0 through a dedicated wire pair to the HI CAL and LO CAL terminals of the preamplifier. Current I_0 has a dc bias component and an ac signal component. The latter is proportional to the CAL INPUT voltage V_i supplied by the user. The controlled current I_0 flows through the input LED of optoisolator IS1. The dc component serves to bias IS1 into the linear portion of its transfer characteristics. The ac component is converted to an ac calibration voltage across R2. This is coupled through Y1 into the preamplifier, simulating an acoustically produced signal. Resistor R4 is a selectable trimmer for I_0 . The circuit is designed so that many identical units can be placed in series and stimulated by the single calibration signal V_i , although only one H78B was used in the VEKA I-A array. A more detailed description of the SARA calibration signal generator circuit was given in conjunction with Fig. 19. Table C1 shows typical performance of the calibration portion of the H78B circuitry.

Table C1 — Typical Performance of the Calibration Circuit in the H78B Preamplifier

Conditions:	
Calibration signal generator ac input:	3.5 V rms
Calibration signal generator dc output:	0.63 mA dc
Frequency:	400 Hz
Temperature:	25°C
Resultant voltage across R2:	60 mV rms
Distortion:	less than 1%

Appendix D

ALTERNATE CALIBRATION METHOD

Early in the developmental phase of the VEKA array project the Acoustics Division of NRL requested that USRD investigate the possibility of placing an on-board signal source with each hydrophone that could be switched-in to calibrate the hydrophone. Switching from the acoustic mode to the calibration mode was to require no additional wires in the VEKA cable. Although the VEKA preamplifier design had not been defined at this point, it was known that it would be a two-wire device; that is, the preamplifier supply current, output signal, and any necessary switching would have to share a single wire pair. This appendix will describe the scheme that was developed as a result of this study. (The requirement for an on-board signal source was later dropped, so that this circuitry was not used in the VEKA array.)

For the purposes of the investigation the general hydrophone/preamplifier configuration shown in Fig. D1 was envisioned for VEKA. It operates as follows: The dc supply current originates at the load supply E_{dc} . It flows through R1 and R2 to zener diodes CR1 and CR2. Diodes CR1 and CR2 form a voltage regulator that produces the dc supply voltage V_{cc} for preamplifier circuit A1. The audio output of A1 passes through capacitors C1 and C2 to the load.

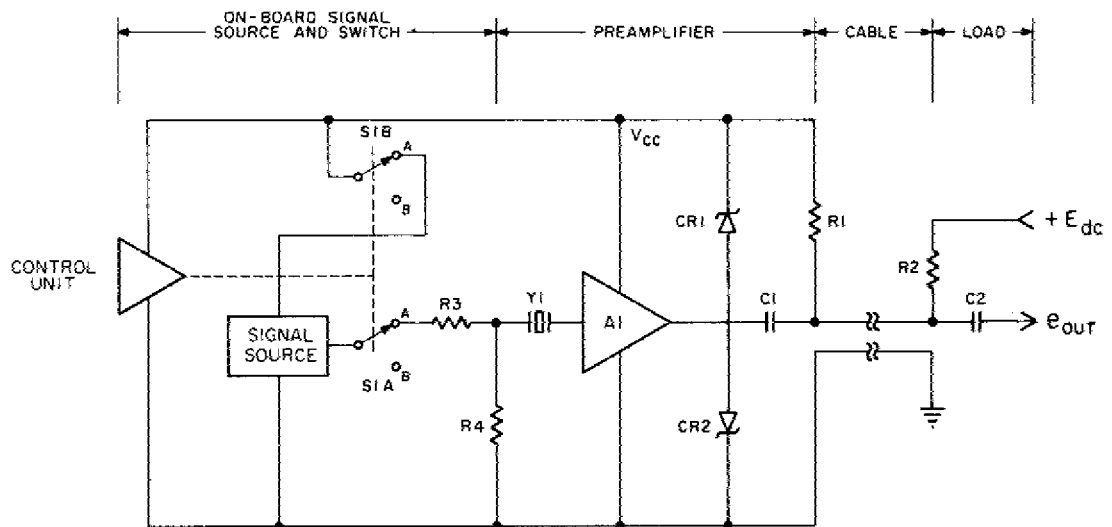


Fig. D1 — General two-wire hydrophone preamplifier system with an on-board signal source

A signal source within the hydrophone, an on-board signal source such as an oscillator, is controlled by relay S1. When S1 is in position A, power is applied to the signal source, and its output is connected through R3 and R4 to Y1. Thus the on-board signal is voltage-divided and placed in series with Y1; this precise input signal allows the hydrophone to be calibrated. When S1 is in position B, power is removed from the signal source. Also, the low end of Y1 is connected through R4 to ground. The hydrophone and preamplifier now operate in the normal acoustic mode. Placing R4 in series with Y1 is not detrimental, since the input impedance of A1 would be much greater than R4. There are several other ways of switching the signal source in or out, but the fundamental problem is finding a means of stimulating relay S1. This can be done as follows: As shown in Fig. D1, the circuit contains two switch sections: S1A and S1B. Both sections switch from position A to B or vice versa simultaneously when stimulated by the control unit. The control unit causes S1A and S1B to switch when V_{cc} goes to zero. This occurs whenever the user removes power at E_{dc} . For example, suppose S1A and S1B are in position A, the case shown in Fig. D1, and that power is on (supply voltage present at E_{dc}). Now the user turns the circuit off by removing the supply voltage at E_{dc} . When this happens, S1A and S1B are switched to position B. They will remain in this position when power is next applied. If power is removed again, they will return to position A and remain there when power is reapplied. Therefore the user can control the switch from the end of the two-wire cable merely by removing and reapplying power.

The control unit and relay were given the name "magnetic flip-flop" by USRD. (A patent application submitted for the magnetic flip-flop has been assigned Navy Case No. 62,151.) A detailed description of this device will now be given.

Figure D2 is a schematic diagram of the magnetic flip-flop. The control unit comprises resistors R1 and R2, capacitors C1 and C2, diodes CR1 and CR2, and relay K2. Relay K1 contains the switch sections S1A and S1B. Relay K1 is a double-pole, double-throw (DPDT) magnetic latching relay with internal diodes as shown in Fig. D2. Relay K2 is a single-pole, double-throw (SPDT) relay in which the normally closed (NC) contacts are used. K2 also contains internal diodes, as shown in Fig. D2, but it is not a latching relay. K2 will operate (switch to an open condition) whenever adequate voltage is applied to its coil. In this application K2 is rated to operate at the V_{cc} potential. However, it will actually operate at approximately $(1/2)V_{cc}$ and can then be sustained in the open condition with only a few volts. The circuit works as follows:

- Assume switch sections S1A and S1B to be in position B, as shown in Fig. D2. Also assume that $V_{cc} = 0$. Therefore, S2 is closed, and capacitors C1 and C2 are completely discharged through S2.
- Now assume that power is applied to the circuit. As V_{cc} begins to rise toward its nominal value, current begins to flow through R1 and coil A, and C1 begins to charge. R1 is chosen so that the voltage across coil A is not enough to operate K1. As V_{cc} continues to rise, S2 opens. Then there is no current flow through coil A, and C1 charges to the full value of V_{cc} .

- To operate K1, V_{cc} is removed (by replacing E_{dc} with either an open circuit or a ground). Capacitor C1 has no discharge path until S2 closes, and this occurs only when V_{cc} is within several volts of ground. When S2 closes, C1 discharges through coil A and S2 to ground. This operates K1, switching S1A and S1B from position B to position A. K1 is now latched in the new state.
- The procedure when power is next applied is as described above except that C2 is charged. When V_{cc} is removed, C2 discharges through coil B, switching S1A and S1B back to position B.

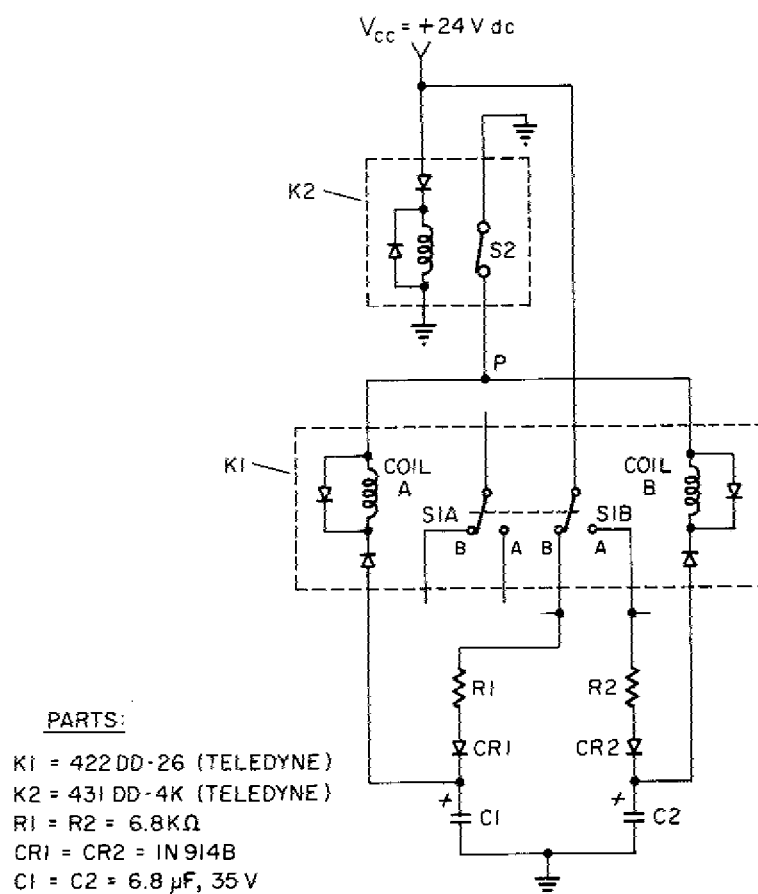


Fig. D2 — Magnetic flip-flop

The circuit of Fig. D2 provides the desired switching functions of Fig. D1 without any additional wires in the hydrophone cable. Switching from position A to B or vice versa will always occur upon removal of power from the circuit. In the VEKA application one might wish to have a means of forcing the magnetic flip-flop into a known state, say position A. This would be useful, since there might be many of the flip-flops in use. The addition of five components, as shown in Fig. D3, accomplishes this. The new components are CR3, CR4, CR5, R3, and transistor Q1. In normal operation, CR 3 and CR5 are backbiased, and Q1 is switched off. The circuit then operates normally, as described above.

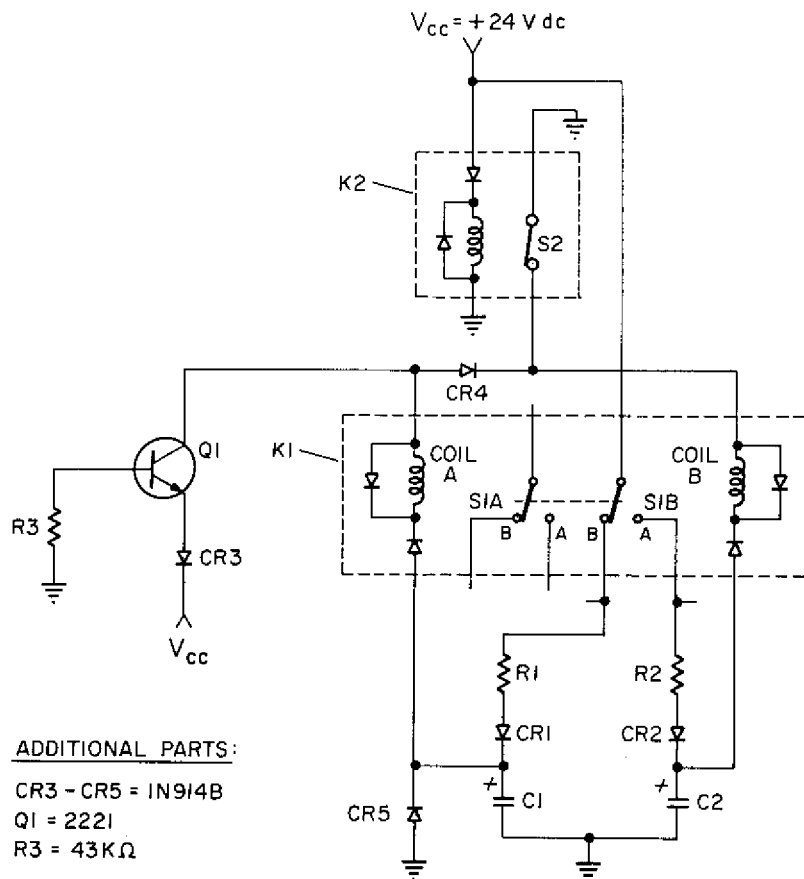


Fig. D3 — Modified magnetic flip-flop

To force K1 to position A, the operator merely reverses E_{dc} and ground (Fig. D1). All of the ground connections in Fig. D3 then become V_{cc} , and all of the V_{cc} connections become ground connections. When this is done:

- Relay K2 is not operated, so S2 remains closed;
- Transistor Q1 is turned on, clamping its collector at a potential near ground;
- Current flows through CR5, coil A, Q1, and CR3 to ground, latching K1 to position A; and
- When power is next applied in the normal fashion, without reversing V_{cc} and ground, K1 will be in this state.

The purpose of diode CR3 is to prevent breakdown of Q1's base-emitter junction when the circuit is connected normally with no power reversal. The purpose of CR4 is to avoid shorting V_{cc} to ground via S2 and Q1 when reversing the power supply.

The basic circuit of Fig. D2 contains only eight components. Relays K1 and K2 are each housed in small TO-5 transistor-type enclosures. The circuit could be manufactured as a potted module. The five additional components of Fig. D3 are optional and would add little to the module size. It is feasible to place all of the components of Fig. D3, excluding the relays and capacitors, into a single hybrid circuit. Operation of this device depends only on the level of V_{cc} . It is affected neither by the length of the hydrophone cable nor by the rise and fall times of V_{cc} .

Under certain conditions the circuit of Fig. D2 can be simplified by removing relay K2 and resistors R1 and R2. This is possible if power is removed by rapidly replacing V_{cc} with a low impedance to ground. Then K2 could be omitted, and point P of Fig. D2 would be connected directly to V_{cc} . With R1 and R2 omitted, S1B contacts B and A would connect directly to CR1 and CR2 respectively.

The magnetic flip-flop circuit of Figs. D2 and D3 was tested successfully as a bread-board. A V_{cc} of ± 24 V dc was arbitrarily chosen for the study but is not critical. With component changes the circuit will operate using other values of V_{cc} .

Appendix E

VEKA I-A PROTOTYPE CABLE

A 14-m length of VEKA I-A prototype cable was furnished to USRD by NORDA for evaluation and to aid in the development of the hydrophones and cone adapters. The cable has 48 twisted pairs of No. 24 AWG stranded copper wire with 0.3-mm-thick (0.010-in.-thick) polyvinyl insulation. There are eight strands of braided Kevlar with six twisted pairs of wire in each strand. The Kevlar strands are braided together in a two-under, two-over pattern, and the assembly is overbraided with a polyester jacket with strum-suppressor fairing.

Figure E1 is a photograph of a section of the prototype cable with a portion of the polyester jacket removed. Figure E2 shows a closer view of the cable with one of the Kevlar strands pulled back to expose the wire pairs. Figure E3 is an end cross-sectional view of the cable.

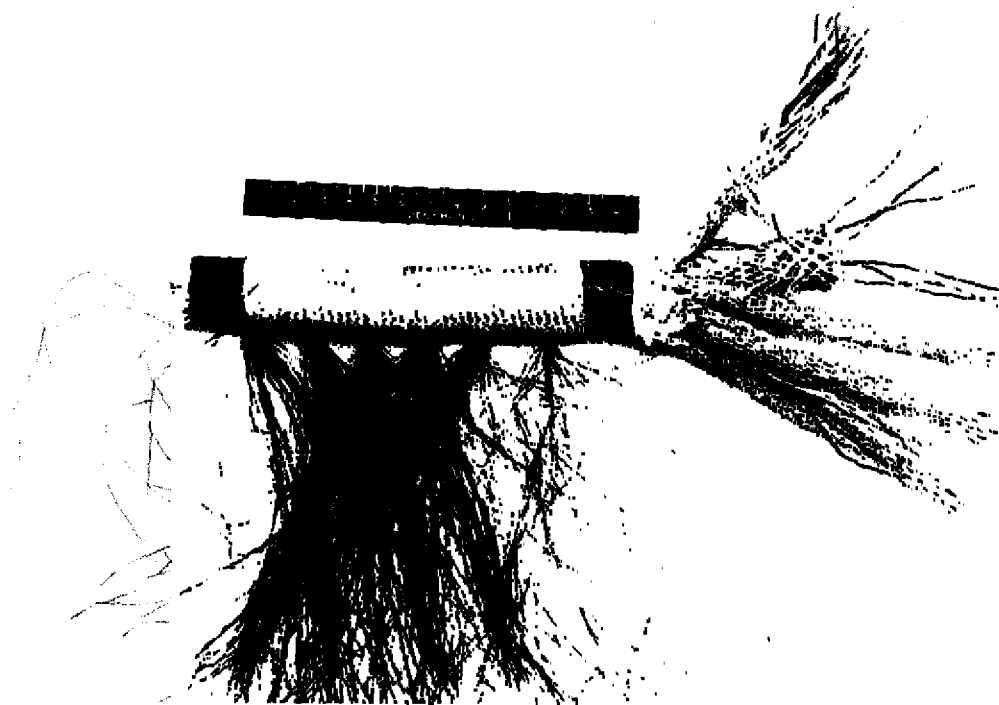


Fig. E1 — Section of prototype cable with portion of polyester jacket removed

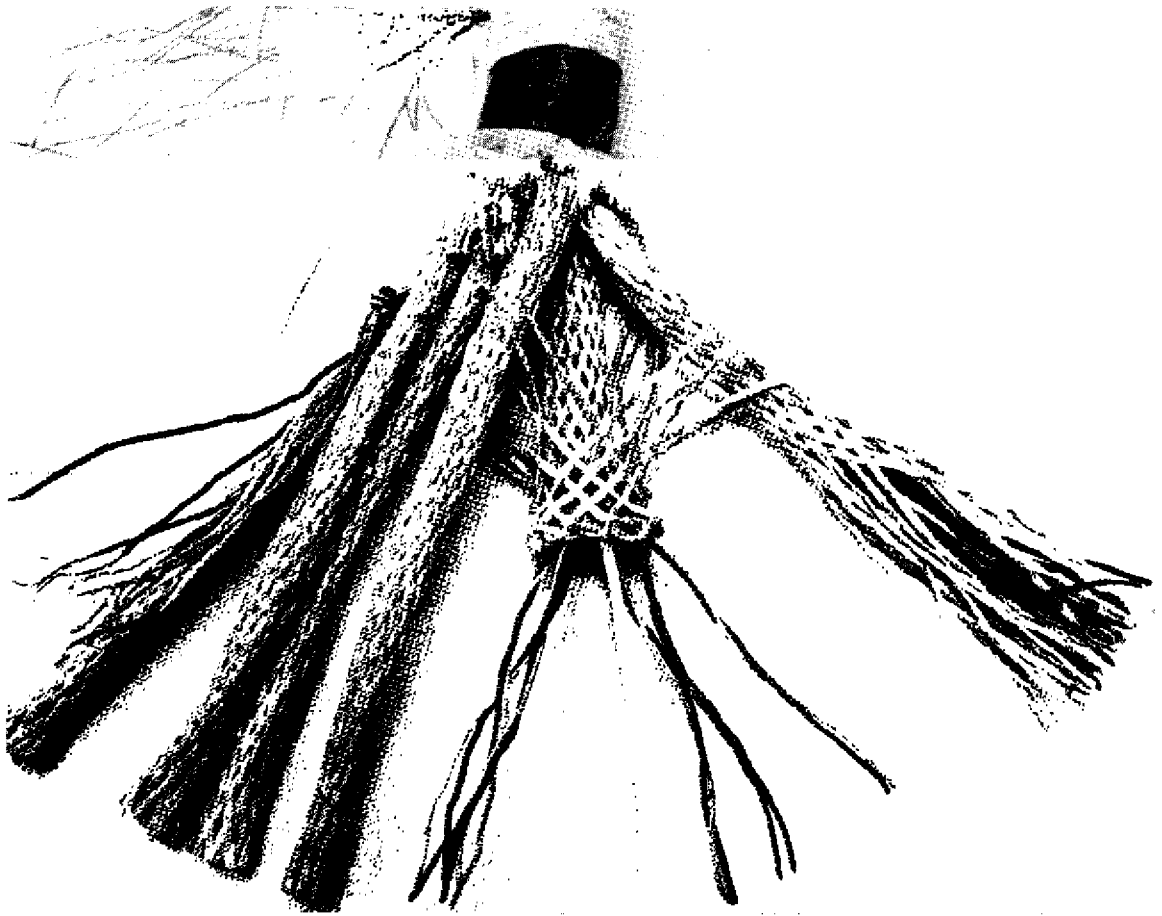


Fig. E2 — Close-up view of cable with one of the Kevlar strands pulled back to expose the electrical conductors



Fig. E3 — End view of cable construction

Appendix F

ANALYSIS OF VEKA I-A CABLE FAILURE

During the hydrophone preamplifier development phase, when the H78B hydrophone preamplifier had been tentatively chosen for use in the VEKA array, the Acoustics Division of NRL requested that USRD analyze the effects of a single failure in the VEKA cable. The cable failures to be considered were the opening of any single conductor and the shorting of any single conductor to any other conductor. The shorting modes to be considered were a direct short and a short through seawater.

The results of the failure analysis are given in Table F1. Figure C1, the H78B preamplifier schematic, is a diagram of a single hydrophone channel showing cable conductors A, B, HI CAL, and LO CAL. In Table F1 subscripts are used to identify conductors for different channels. Although 1 and 2 are the only subscripts used, they do not necessarily denote channels 1 and 2 only; they denote any two channels. For example "B₁ shorts to LO CAL₂" means conductor B in one array channel shorts to the LO CAL conductor in another channel. "A₁ shorts to B₁" means that conductor A in one array channel shorts to conductor B in the same channel.

Table F1 -- Effects of VEKA Cable Failure

Failure Mode	Short-Circuit Mode		Effect
	Direct	Through H ₂ O	
1. A ₁ opens			Channel 1 is lost; other channels are unaffected.
2. B ₁ opens			Channel 1 is lost; other channels are unaffected.
3. HI CAL ₁ opens			The calibration function is lost for all channels.
4. LO CAL ₁ opens			The calibration function is lost for all channels.
5. HI CAL ₁ shorts to LO CAL ₁	X		The calibration function is lost for channel 1 only; other channels are unaffected.
6. HI CAL ₁ shorts to LO CAL ₁		X	Channel-1 calibration output signal may become distorted due to the shunting effect of seawater; other channels are unaffected.

Table continues.

Table F1 (Continued) — Effects of VEKA Cable Failure

Failure Mode	Short-Circuit Mode		Effect
	Direct	Through H ₂ O	
7. A ₁ shorts to B ₁	X		Channel 1 is lost; the receiver input resistor for channel 1 will burn out unless the fuse blows on the +36-V dc power supply.
8. A ₁ shorts to B ₁		X	The dc level at the input of receiver channel 1 rises or is erratic; if it is erratic, the erraticity will appear (amplified by 67 dB) at the output of receiver channel 1.
9. A ₁ shorts to A ₂	X	X	Some slight crosstalk appears between the channel-1 and channel-2 outputs.
10. A ₁ shorts to B ₂	X		Similar to item 7; channel 2 is lost, and the input resistor of receiver channel 2 possibly is damaged.
11. A ₁ shorts to B ₂		X	Similar to item 8, except that channel 2 is affected.
12. A ₁ shorts to HI CAL ₁ , LO CAL ₁ , HI CAL ₂ , or LO CAL ₂	X		At least one of the calibration LEDs probably opens, eliminating the calibration function for the whole array, but the array still operates acoustically.
13. A ₁ shorts to HI CAL ₁ , LO CAL ₁ , HI CAL ₂ , or LO CAL ₂		X	Some or all of the calibration output signals possibly become distorted, but the array still operates acoustically.
14. B ₁ shorts to B ₂	X	X	The channel-1 and channel-2 output signals become mixed.

Table continues.

Table F1 (Continued) — Effects of VEKA Cable Failure

Failure Mode	Short-Circuit Mode		Effect
	Direct	Through H ₂ O	
15. B ₁ shorts to HI CAL ₁ , LO CAL ₁ , HI CAL ₂ , or LO CAL ₂	X		If the short occurs electrically close to the -45-V dc level on the calibration line, the channel-1 transmitter and receiver both become damaged; also, the calibration line probably fails, as in item 12.
16. B ₁ shorts to HI CAL ₁ , LO CAL ₁ , HI CAL ₂ , or LO CAL ₂		X	If the short occurs electrically close to the -45-V dc level on the calibration line, the channel-1 transmitter possibly is damaged; the channel-1 receive signal possibly becomes erratic, and the calibration signal outputs possibly become distorted.
17. HI CAL ₁ shorts to HI CAL ₂	X		The calibration function is lost for all channels bypassed by the short, but acoustic operation remains normal.
18. HI CAL ₁ shorts to HI CAL ₂		X	The calibration function becomes distorted for all channels bypassed by the short, but acoustic operation remains normal.
19. HI CAL ₁ shorts to LO CAL ₂	X		The calibration function is lost for all channels bypassed by the short, but acoustic operation remains normal.
20. HI CAL ₁ shorts to LO CAL ₂		X	The calibration function becomes distorted for all channels bypassed by the short, but acoustic operation remains normal.

Table continues.

Table F1 (Concluded) — Effects of VEKA Cable Failure

Failure Mode	Short-Circuit Mode		Effect
	Direct	Through H_2O	
21. LO CAL ₁ shorts to LO CAL ₂	X		The calibration function is lost for all channels bypassed by the short, but acoustic operation remains normal.
22. LO CAL ₁ shorts to LO CAL ₂		X	The calibration function becomes distorted for all channels bypassed by the short, but acoustic operation remains normal.